Wave reflection by a flat plate cascade

by

Pieter Jan Grooth

Civilingenjör, Chalmers University of Technology
Göteborg, Sweden
(1987)

SUBMITTED IN PARTIAL FULFILLMENT OF THE
REQUIREMENTS FOR THE DEGREE OF
Master of Science
in
Aeronautics and Astronautics
at the
Massachusetts Institute of Technology

September 1990

Signature of Author _____
Department of Aeronautics and Astronautics
August 10, 1990

Certified by _____
Professor Mårten T. Landahl
Thesis Supervisor, Department of Aeronautics and Astronautics

Accepted by _____
Professor Harold Y. Wachman
Chairman, Department Graduate Committee

Wave reflection by a flat plate cascade

by

Pieter Jan Grooth

Submitted to the Department of Aeronautics and Astronautics

on August 10, 1990

in partial fulfillment of the requirements for the degree of

Master of Science in Aeronautics and Astronautics

Abstract

Reflection of plane waves in a compressible flowing fluid, by a two-dimensional flat plate cascade, is considered. The aim of this analysis is to develop a model for wave reflection that can be incorporated in unsteady flow calculations for vibrating compressor blades. By use of kernel function formulation for the cascade in combination with expressions for the pressure jump across a semi-infinite flat plate subject to a plane incident wave approximate expressions for the reflection coefficients of pressure waves and vorticity waves are derived These reflection coefficients have been found to be in good agreement with those calculated by using the semi-actuator disk theory of Kaji and Okazaki (1970a). Unlike the semi-actuator disk theory the reflection coefficients derived here can handle both subresonant (i.e only the lowest wave mode is propagating) and superresonant (i.e more modes than the lowest wave modes propagates) cases.

Thesis Supervisor: Mårten T. Landahl

Professor of Aeronautics and Astronautics

Acknowledgements

I would like to thank Professor Mårten Landahl for his guidance and support throughout this work. I would also like to express my gratitude to Professor Christian Högfors and Professor Anders Boström who contibuted to make it possible for me to come to MIT.

This work was supported by Volvo Flygmotor AB.

Contents

List of Figures

NOMENCLATURE

a	speed of sound
c	chord length
G	Green's function
h	tangential wave number of the incident wave
$H^{(2)}$	Hankel function of the second kind
k	axial wave number of the incident wave
K	kernel function
K_p	kernel function for the pressure field
K_w	kernel function for the upwash
K_ϕ	irrotational part of K_w
K_ψ	rotational part of K_w
M	mean flow Mach number
M_x	axial Mach number
M_y	tangential Mach number
p	pressure perturbation
$\bar{p}$	defined by $p = \bar{p}(x, \bar{y})e^{i(\lambda t + \kappa M x)}$
Δp	pressure jump
P	$-\frac{1}{\beta}\frac{\partial}{\partial y}p^{inc}(x, y_1)$
R	reflection coefficient
S	blade spacing
t	nondimensional time
T	transmission coefficient
u	axial velocity perturbation
$\bar{u}$	axial mean velocity
v	tangential velocity perturbation
$\bar{v}$	tangential mean velocity
w	velocity nomal to the blade surface
W	magnitude of the mean velocity

x, y	coordinate system shown in figure 1.1
x_1, y_1	coordinate system shown in figure 1.1
X, Y	coordinate system shown in figure 5.1
X_1, Y_1	coordinate system shown in figure 5.1
$\bar{y}$	$y\sqrt{1-M^2}$

α	axial wave number
β	$\sqrt{1-M^2}$
β_x	$\sqrt{1-M_x^2}$
γ	streamwise wave number
η	source coordinate
θ	angle of stagger
κ	$\frac{\lambda M}{\beta^2}$
λ	reduced frequency
μ	tangential wave number
ν	$\gamma - \kappa M$
ξ	source coordinate see figure 1.1
ρ	density perturbation
$\bar{\rho}$	mean density
σ	interblade phase angle
ϕ	velocity potential
$\Delta\phi$	jump in velocity potential

Subscript

c	field inside the cascade
d	field downstream of the cascade
i	imaginary part

NR	normal to rotor blade
NS	normal to stator blade
pres	prescribed
r	real part
s	stator
SF	space fixed
u	field upstream of the cascade
I	case 1
II	case 2
III	case 3
1	refers to upstream propagating pressure wave
2	refers to downstream propagating pressure wave
3	refers to vorticity wave

Superscript

inc	incident
m	m:th harmonic
ref	reflected
$\hat{}$	amplitude

Chapter 1
Introduction

The problem considered in this thesis is wave reflection by cascades, for application to unsteady flow in axial flow compressors.

Background

The turbomachine is inherently unsteady. This unsteadiness is the cause of sound wave generation and fluctuating aerodynamic forces on the blading, both of which are of great concern in designing engines. These fluctuating forces may interact with the structure to give a self sustained oscillation with growing amplitude; flutter. The sound waves generated by an oscillating rotor blade row may be partly reflected back by a neighboring stator blade row and give rise to forces that change the aerodynamic damping of the rotor. Our knowledge of the various unsteady phenomena in turbomachinery is limited. In the design process of turbomachines this lack of insight is compensated for by rules of thumb based on experience. Demands of higher performance and less weight has lead to design trends with higher mass flux and more slender blade profiles. The more slender profile is more flexible than a thicker profile and it is therefore expected to flutter at lower fluid velocity than the thicker profile. This have increased the problem with flutter and made it necessary to acquire deeper insight into unsteady phenomena in turbomachines in order to carry the development of turbomachines further. To gain this insight an essential part is the development of unsteady aerodynamic models. Development of such models require a lot of approximations and simplifications due to the complexity of the flow field.

Previous work

The last 20 years a number of simplified aerodynamic models for compressible flow

have been developed. Among these is the flat plate cascade model. In the model the blade row consists of an infinite number of parallel flat plates. The flow field is a steady uniform mean flow upon which small perturbation are superimposed. The governing equations are linearized about the uniform mean flow and the small perturbations are solved for. This model may be regarded as an extension of the incompressible theory developed by Whitehead (1962). Kernel functions and integral equations for the flat plate cascade in subsonic flow have been derived by Kaji and Okazaki (1970b). They used the model for wave reflection. But, the first complete analysis of subsonic flow, together with numerical method for the solution of the integral equation, is due to Smith (1971). Ni (1979) extended the model for supersonic flutter analysis.

The development of more powerful computers have made it possible to do unsteady simulations based on the Euler equations and the Navier-Stokes equations. Elaborate codes with solution adaptive grid for two-dimensional flow have been developed by Sidén (1990). A simulation for one blade passage with such a code take several hours on a mini-supercomputer. The two models mentioned above may be regarded as extremes. The first is too simple for loaded blades. The limitation for the second is set by the available computers. The long computational time for unsteady Euler and Navier-Stokes solvers suggests that these have to be combined with more simplified models to include effects of for example neighboring blade rows in order to arrive at a reasonable computational cost.

Present work

This work has been focused on wave reflection in blade rows. Waves generated by an oscillating rotor blade may be partially reflected back by neighboring a stator blade row. In linear analyses based on small perturbations the amplitude of the reflected waves may be of the same order as the emitted waves. This suggests that forces induced by the reflected waves can not be neglected in such analyses. In more advanced computer codes the upstream and downstream boundary conditions are often of a nonreflecting type. By introduction of reflection coeffients at these boundaries one may at least get a 'flavor' of the presence of neighboring balde rows.

In the model considered here the reflection coefficients are derived for a flat plate cascade. The pressure jump across a semi-infinite flat plate due to plane incident waves is calculated. This pressure jump is used in the kernel function formulation for the flat plate cascade as loading on the blades.

The flat plate cascade is presented in chapter 2. In chapter 3 the pressure jump across a semi-infinite flat plate is derived. The result from chapters 2 and 3 are used in chapter 4 to derive expressions for the reflection coefficients. A comparison between these and reflection coefficients obtained by the use of semi-actuator disk theory is also carried out in chapter 4. In chapter 5 some applications of the reflection coefficients are outlined.

Chapter 2

The flat plate cascade model

In this chapter the flat plate cascade model is presented. It has previously been applied to various problems; sound generation Smith (1971), propagtion of sound waves in compressors Kaji and Okazaki (1970b), flutter in supersonic flow Ni (1979). The model is used in a later chapter to derive reflection coefficients for pressure and vorticity waves.

2.1 The model and its governing equations

The flat plate cascade consists of an infinite number of flat plates, with an angle of stagger θ (see figure 1.1, page 15). Through the cascade an inviscid perfect gas is flowing with uniform mean velocity, W, and uniform entropy. The velocity W is assumed to be parallel to the cascade blades, so there is no steady lift on the blades.

All of the flow quantities; velocity, pressure and density, are assumed to consist of a steady undisturbed part and a small time-dependent perturbation. For example the pressure is: $\bar{p}+p$, where the barred quantity is the undisturbed part and the unbarred quantity is the unsteady perturbation. By substitution of these expressions into the continutity equation and the momentum equation, then linearizing the equations by neglecting terms of second order in perturbation quantities one finds the following linearized continuity and momentum equations:

$$\frac{D\rho}{Dt} + \bar{\rho}\left(\frac{\partial u}{\partial x} + \frac{\partial v}{\partial y}\right) = 0 \tag{2.1}$$

$$\frac{Du}{Dt} = -\frac{1}{\bar{\rho}}\frac{\partial p}{\partial x} \tag{2.2}$$

$$\frac{Dv}{Dt} = -\frac{1}{\bar{\rho}}\frac{\partial p}{\partial y} \tag{2.3}$$

where

$$\frac{D}{Dt} = \frac{\partial}{\partial t} + \bar{u}\frac{\partial}{\partial x} + \bar{v}\frac{\partial}{\partial y}$$

and p, ρ, u and v are the unsteady perturbations of pressure, density, and velocity in the x- and the y-direction, respectively. The barred variables denote steady quantities. The isentropic relation

$$p = a^2\rho \tag{2.4}$$

where a^2 is the speed of sound, completes the set of governing equations for the model.

The governing equations may be written in non-dimensional form by introduction of the following non-dimensional variables:

$$x^* = \frac{x}{c}, \quad t^* = \frac{Wt}{c}, \quad \rho^* = \frac{\rho}{\bar{\rho}}, \quad u^* = \frac{u}{W}, \quad p^* = \frac{p}{\bar{\rho}W^2}$$

where star denotes non-dimensional variables. Substitution of these into the governing equations and the dropping of the stars gives the following equations:

$$\frac{\partial \rho}{\partial t} + \frac{\partial \rho}{\partial x}\cos\theta + \frac{\partial \rho}{\partial y}\sin\theta + \frac{\partial u}{\partial x} + \frac{\partial v}{\partial y} = 0 \tag{2.5}$$

$$\frac{\partial u}{\partial t} + \frac{\partial u}{\partial x}\cos\theta + \frac{\partial u}{\partial y}\sin\theta = -\frac{\partial p}{\partial x} \tag{2.6}$$

$$\frac{\partial v}{\partial t} + \frac{\partial v}{\partial x}\cos\theta + \frac{\partial v}{\partial y}\sin\theta = -\frac{\partial p}{\partial x} \tag{2.7}$$

$$\rho = M^2 p \tag{2.8}$$

From these equations the wave equation for the perturbation pressure is deduced and its Green's function found. The Green's function is then used to derive kernel functions for upwash integral for the cascade. From the upwash integral and the boundary condition of no flow through the blade, the unsteady loading may be obtained.

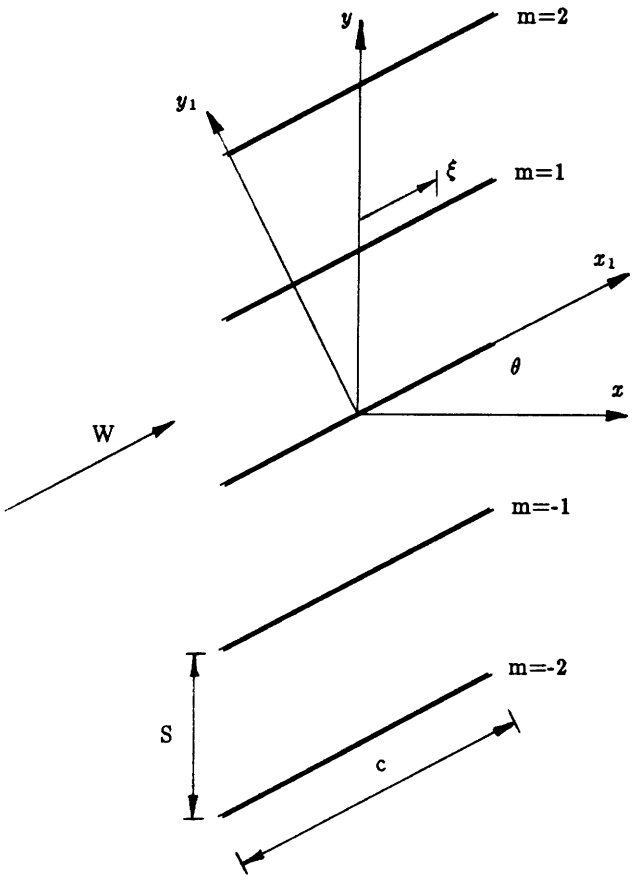

Figure 2.1: Cascade model

2.2 Wave equation and Green's function

With the introduction of a new coordinate system (see figure 1.1) with the x_1-axis parallel to the blade surface and the y_1-axis normal to the blades one finds that the governing equations are:

$$\frac{\partial \rho}{\partial t} + \frac{\partial \rho}{\partial x_1} + \frac{\partial u_1}{\partial x_1} + \frac{\partial v_1}{\partial y_1} = 0$$

$$\frac{\partial u_1}{\partial t} + \frac{\partial u_1}{\partial x_1} = -\frac{\partial p}{\partial x_1}$$

$$\frac{\partial v_1}{\partial t} + \frac{\partial v_1}{\partial x_1} = -\frac{\partial p}{\partial y_1}$$

$$\rho = M^2 p$$

where u_1 and v_1 are the velocity components in the x_1- and the y_1-direction, respectively. By eliminating ρ, u_1 and v_1 from these equations a wave equation for the pertubation pressure is obtained

$$\beta \frac{\partial^2 p}{\partial x_1^2} + \frac{\partial^2 p}{\partial y_1^2} - 2M^2 \frac{\partial^2 p}{\partial t \partial x_1} - M^2 \frac{\partial^2 p}{\partial t^2} = 0 \tag{2.9}$$

where $\beta^2 = 1 - M^2$.

In the following assume that the pressure has a harmonic temporal dependency, i.e $p \propto e^{i\lambda t}$. The Green's function for the wave equation can be obtained by intoducing one new independent variable $\bar{y}_1$ and a new dependent variable $\bar{p}$ defined by

$$p = \bar{p} e^{i\kappa M x_1} \quad \text{and } \bar{y}_1 = \beta y_1$$

where $\kappa = \frac{\lambda M}{\beta^2}$. By substituting $\bar{p}$ and $\bar{y}_1$ in the wave equation Helmholtz' equation is obtained:

$$\frac{\partial^2 \bar{p}}{\partial x_1^2} + \frac{\partial^2 \bar{p}}{\partial \bar{y_1}^2} + \kappa^2 \bar{p} = 0 \tag{2.10}$$

which has a Hankel function of order zero as Green's function. The requirement of outgoing waves in the far field implies that the Hankel function of the second kind should be chosen. This leads to the following Green's function for the wave equation:

$$G(x_1, y_1, \xi, \eta) = \frac{i}{4\beta} H_0^{(2)}(\kappa r) e^{i\kappa M(x_1 - \xi)} \tag{2.11}$$

where

$$r = \sqrt{(x_1 - \xi)^2 + \beta^2 (y_1 - \eta)^2}$$

and ξ and η are the source coordinates.

2.3 Pressure field and upwash

The pressure field due to a cascade blade subject to vibration or oncoming waves can be expressed as an integral over the blade surface of pressure doublets. This distribution of doublets is given by the pressure jump across the blade times the normal derivative of the Green's function.

Let the source point on the m:th blade be

$$\xi_m = \xi + mS \sin\theta \quad \text{and} \quad \eta_m = mS \cos\theta$$

where θ is the angle of stagger and S is the blade spacing, and ξ is measured from midchord on each blade paralell to the x_1-axis. The assumption that the pressure jump for adjacent blades differs only by a constant phase angle, σ, leads to an expression for the field from the whole cascade in terms of the pressure jump across the zeroth blade

$$p(x_1, y_1) = \int_{-\frac{1}{2}}^{\frac{1}{2}} K_p(x_1, y_1, \xi) \Delta p(\xi)\, d\xi \tag{2.12}$$

where

$$K_p(x_1, y_1, \xi) = \sum_{m=-\infty}^{\infty} \frac{\partial G}{\partial \eta}(x_1, y_1, \xi_m, \eta_m) e^{i\sigma m} \tag{2.13}$$

Integrating the momentum equation along the undisturbed streamlines from $-\infty$ to the field point of interest gives the upwash induced by the pressure doublets. From an isolated airfoil the upwash at infinity vanishes , but for a cascade the induced upwash has a finite value. This mean that the value of the upwash far upstream has to be evaluated. The common practice to get around this problem is to assume that the frequency has a small negative imaginary part

$$\lambda = \lambda_r - i\lambda_i,$$

so that all perturbation quantities vanish at infinity. Then, integration of the pressure field from $-\infty$ with the limiting operation $\lim_{\lambda_i \to 0} \lambda$ gives the upwash $w(x_1, y_1)$

$$w(x_1, y_1) = -e^{-i\lambda x_1} \int_{-\infty}^{x_1} e^{i\lambda x_1'} \frac{\partial \hat{p}}{\partial y_1} \, dx_1' \tag{2.14}$$

Substituting the equation for the pressure in the upwash integral leads to

$$w(x_1, y_1) = \int_{-\frac{1}{2}}^{\frac{1}{2}} K_w(x_1, y_1, \xi) \Delta p(\xi) \, d\xi \tag{2.15}$$

where

$$K_w(x_1, y_1, \xi) = -e^{-i\lambda x_1} \int_{-\infty}^{x_1} \sum_{m=-\infty}^{\infty} \frac{\partial^2 G_m}{\partial y_1 \partial \eta} e^{i\lambda x_1' + i\sigma m} \, dx_1' \tag{2.16}$$

The kernel functions K_p and K_w have been derived by Kaji and Okazaki (1970b) (see Appendix A), Smith (1971) and Ni (1979). Through the use of different methods these authors derived expressions all of which can be written in the following forms:

For a *point upstream of* the *doublet* the kernel functions for the pressure and for the upwash are:

$$K_p = -\sum_{n=-\infty}^{\infty} \frac{\mu_n \cos\theta - \alpha_{n1} \sin\theta}{S\beta_x^2(\alpha_{n2} - \alpha_{n1})} e^{i(\alpha_{n1}\cos\theta + \mu_n \sin\theta)(x_1 - \xi) - i(\alpha_{n1}\sin\theta - \mu_n \cos\theta)y_1} \tag{2.17}$$

$$K_w = \sum_{n=-\infty}^{\infty} \frac{(\mu_n \cos\theta - \alpha_{n1} \sin\theta)^2}{S\beta_x^2(\alpha_{n2} - \alpha_{n1})(\lambda + \alpha_{n1}\cos\theta + \mu_n \sin\theta)} \times$$

$$\times e^{i(\alpha_{n1}\cos\theta+\mu_n\sin\theta)(x_1-\xi)-i(\alpha_{n1}\sin\theta-\mu_n\cos\theta)y_1} \tag{2.18}$$

where

$$\mu_n = \frac{2\pi n+\sigma}{S}$$

$$\alpha_{n1} = \frac{1}{\beta_x^2}\{M_x(M_y\mu_n+\lambda M) - i\sqrt{\beta_x^2\mu_n^2-(M_y\mu_n+\lambda M)^2}\}$$

and

$$\beta_x^2 = 1-M_x^2$$
$$M_x = M\cos\theta \quad \text{and} \quad M_y = M\sin\theta$$

for $(x_1-\xi)\cos\theta - y_1\sin\theta < 0$. These kernel functions give the upstream propagating pressure wave and normal velocity associated with this wave, respectively. For a ***point downstream of*** the ***doublets*** the kernel functions are:

$$K_p = -\sum_{n=-\infty}^{\infty}\frac{\mu_n\cos\theta-\alpha_{n2}\sin\theta}{S\beta_x^2(\alpha_{n2}-\alpha_{n1})}e^{i(\alpha_{n2}\cos\theta+\mu_n\sin\theta)(x_1-\xi)-i(\alpha_{n2}\sin\theta-\mu_n\cos\theta)y_1} \tag{2.19}$$

$$K_w = K_\phi + K_\psi \tag{2.20}$$

$$K_\phi = \sum_{n=-\infty}^{\infty}\frac{(\mu_n\cos\theta-\alpha_{n2}\sin\theta)^2}{S\beta_x^2(\alpha_{n2}-\alpha_{n1})(\lambda+\alpha_{n2}\cos\theta+\mu_n\sin\theta)}e^{i(\alpha_{n2}\cos\theta+\mu_n\sin\theta)(x_1-\xi)}\times$$

$$\times e^{-i(\alpha_{n2}\sin\theta-\mu_n\cos\theta)y_1} \tag{2.21}$$

$$K_\psi = -\sum_{n=-\infty}^{\infty}\frac{\lambda^2\cos\theta}{S(\lambda^2+\mu_n^2+2\lambda\mu_n\sin\theta)}e^{-i\lambda(x_1-\xi)+i\frac{\lambda\sin\theta+\mu_n}{\cos\theta}y_1} \tag{2.22}$$

where

$$\alpha_{n2} = \frac{1}{\beta_x^2}\{M_x(M_y\mu_n+\lambda M) + i\sqrt{\beta_x^2\mu_n^2-(M_y\mu_n+\lambda M)^2}\}$$

for $(x_1-\xi)\cos\theta - y_1\sin\theta > 0$. K_p and K_ϕ represent a downstream propagating pressure wave and the normal velocity associated with this wave, respectively. K_ψ represents the kernel for a vorticity wave. This wave convects downstream with the undisturbed free stream velocity.

From the expressions for α_{n1} and α_{n2} one can conclude that for an axial Mach number less than one, i.e. $M_x < 1$, only a finite number of wave modes can propagate. These propagating wave modes have a wave number μ_n that satisfy the following condition

$$-\frac{\lambda M}{\beta_x + M} < \mu_n < \frac{\lambda M}{\beta_x - M} \tag{2.23}$$

If this condition is not satisfied, the wave is of a decaying type and it is said to be suject to cutoff.

In a practical problem one combines the boundary condition that the normal velocity on the blade surface is zero and the upwash integral (2.15) to solve for the pressure distribution on the zeroth blade. To express this mathematically let w_{pres} be the normal velocity due to a prescribed oscillation of the blade or an oncoming wave, the

$$w(x_1, 0) + w_{pres}(x_1, 0) = 0$$

is the relation from which the pressure distribution can be solved for. This has to be done numerically and takes approximately one CPU minute on a MicroVax.

Chapter 3

The pressure jump across a semi-infinite plate

In this chapter expressions for the pressure jump across a semi-infinite plate due to incident waves are derived. These may be used in equations (2.12) and (2.15) as approximations for the loading on the cascade blades to calculate the reflection coefficients.

When a cascade blade is modeled as a semi-infinite plate the loading will differ depending on whether a wave is incident on the leading edge or the trailing edge. In the following the problem is split up into two problems the trailing edge problem and the leading edge problem.

3.1 The trailing edge problem

Consider a semi-infinite plate located at $x \leq 0$, $y = 0$ with a mean flow directed in the positive x-direction. The assumption that the velocity, the pressure and the density can be split into two parts - a steady mean quantity and an unsteady perturbation - leads to the following boundary value problem for the perturbation pressure:

$$\beta^2 \frac{\partial^2 p}{\partial x^2} + \frac{\partial^2 p}{\partial y^2} = M^2 \frac{\partial^2 p}{\partial t^2} + 2M^2 \frac{\partial^2 p}{\partial t \partial x}$$

$$\frac{\partial p}{\partial y} = 0 \quad \text{for } x \leq 0$$

$$p = 0 \text{ for } x > 0$$

In this problem the perturbation pressure is split into one part due to the incident wave and one part due to the diffracted wave. Moreover, the assumption that the pressure perturbation is a harmonic function of time leads to the following boundary value for the diffracted wave:

$$\frac{\partial^2 \bar{p}}{\partial x^2} + \frac{\partial^2 \bar{p}}{\partial \bar{y}^2} + \kappa^2 \bar{p} = 0 \tag{3.1}$$

$$\frac{\partial \bar{p}}{\partial \bar{y}} = P(x) e^{-i\kappa x} \text{ for } x \leq 0 \tag{3.2}$$

$$\bar{p} = 0 \quad \text{for} \quad x > 0 \tag{3.3}$$

where

$$\bar{y} = \beta y, \quad \kappa = \frac{\lambda M}{1 - M^2}, \quad p = \bar{p}(x, \bar{y}) e^{i(\lambda t + \kappa M x)}$$

and

$$P(x) = -\frac{1}{\beta} \frac{\partial}{\partial y} p^{inc}(x, y) \quad \text{for } y = 0$$

This problem can be solved by using a method first introduced by Landahl (1961). The idea in this method is to construct a kernel function such that its normal derivative is a delta funtion for $x \leq 0$, zero for $x > 0$ and to express the solution as an integral.

$$\bar{p} = \int_{-\infty}^{0} K(x - \xi)\, P(\xi)\, d\xi$$

To do this, introduce polar coordinates r and φ where φ is measured clockwise from the negative x -axis, so that

$$x = -r \cos \varphi \quad \text{and } \bar{y} = r \sin \varphi$$

Then, a solution $\bar{p} = \chi$ satisfying equations (3.1) and (3.3) and vanishing at infinity can be found by separation of variables to be

$$\chi = cos(\frac{\varphi}{2}) H_{\frac{1}{2}}^{(2)}(\kappa r) = i\, cos(\frac{\varphi}{2}) \sqrt{\frac{2}{\pi \kappa r}} e^{-i\kappa r} \tag{3.4}$$

χ can be used to construct a solution $\bar{p} = \chi_0$ such that, for $x < 0$, $\bar{y} = +0$

$$\frac{\partial \chi_0}{\partial \bar{y}} = e^{isx}$$

Such a solution is given by

$$\chi_0 = A\int_x^\infty e^{is(x-x_1)}\chi(x_1,\bar{y})\,dx_1 \tag{3.5}$$

where A is determined from the requirement that $\frac{\partial\chi_0}{\partial\bar{y}} = e^{isx}$ on the negative x-axis. Extraction of the fundamental singularity and straight forward integration leads to

$$A = \frac{1+i}{2}\sqrt{\frac{\kappa}{s+\kappa}}$$

Now, the solution for $\bar{p}$ can be obtained from χ_0 as

$$\bar{p} = \frac{1}{2\pi}\int_{-\infty}^{\infty}\chi_0\,ds\int_{-\infty}^{0}P(\xi)\,e^{-is\xi}d\xi \tag{3.6}$$

Substitution of the expression for χ_0 into the above equation leads to the following equation for $\bar{p}$ on the negative x-axis:

$$\bar{p} = \frac{i-1}{2\pi}\int_{-\infty}^{\infty}\frac{e^{is(x-x_1-\xi)}}{\sqrt{\kappa+s}}\,ds\int_x^0\frac{e^{i\kappa x_1}}{\sqrt{2\pi(-x_1)}}\,dx_1\int_{-\infty}^{0}P(\xi)\,d\xi \tag{3.7}$$

The integration over s can be carried out first giving

$$I = \int_{-\infty}^{\infty}\frac{e^{is(x-x_1-\xi)}}{\sqrt{\kappa+s}}\,ds$$

Before evaluating I note that the assumption of $Im(s+\kappa) = Im(\kappa) < 0$, makes the integral converge at its upper limit. Now, substitution of $z = i(s+\kappa)$ into I leads to

$$I = 2\pi e^{-i\kappa(x-x_1-\xi)+i\frac{\pi}{4}}\left(\frac{1}{2\pi i}\int_{-i\infty+\kappa_i}^{i\infty+\kappa_i}\frac{dz}{\sqrt{z}}e^{z(x-x_1-\xi)}\right) \tag{3.8}$$

where $\kappa_i = -Im(\kappa)$. If $x - x_1 - \xi > 0$, then the factor within parantheses can be recognized as the inverse Laplace transform of $\frac{1}{\sqrt{z}}$ so that

$$I = \begin{cases} (1+i)\sqrt{\frac{2\pi}{x-x_1-\xi}}e^{-i\kappa(x-x_1-\xi)} & \text{for } x-x_1-\xi > 0 \\ 0 & \text{for } x-x_1-\xi < 0 \end{cases}$$

Substitution of this result into equation (3.7) leads to

$$\bar{p}(x,+0) = -\frac{1}{\pi}\int_{-\infty}^{0}P(\xi)K(x,\xi)\,d\xi \tag{3.9}$$

where

$$K(x,\xi) = \int_x^{x_0} \frac{e^{-i\kappa(x-2x_1-\xi)}}{\sqrt{-x_1(x-x_1-\xi)}}\, dx_1 \tag{3.10}$$

and

$$x_0 = \begin{cases} 0 & \text{for } \xi < x \\ x-\xi & \text{for } \xi > x \end{cases}$$

By introducing

$$\tau = \frac{x-\xi}{|\,x-\xi\,|} - \frac{2\,x_1}{|\,x-\xi\,|}$$

one may express $K(x,\xi)$ as

$$K(x,\xi) = \int_1^{-\frac{x+\xi}{|x-\xi|}} \frac{e^{-i\kappa|x-\xi|\tau}}{\sqrt{\tau^2-1}}\, d\tau \tag{3.11}$$

Substituting eq.(3.11) into eq.(3.9), assuming that the incident wave is a plane wave, i.e $P(\xi) = \hat{P}e^{i\gamma\xi}$, and reversing the order of integration we find

$$\bar{p}(x,+0) = -\frac{1}{\pi}\hat{P}\int_{\frac{\tau+1}{\tau-1}x}^{\frac{\tau-1}{\tau+1}x} e^{-i\kappa|x-\xi|\tau+i\gamma\xi} d\xi \int_1^{\infty} \frac{1}{\sqrt{\tau^2-1}} d\tau \tag{3.12}$$

Integration with respect to ξ results in

$$\bar{p} = -\frac{1}{\pi}\hat{P}(e^{i\nu x}(I_1+I_2) + I_3 + I_4) \tag{3.13}$$

where

$$I_1 = \int_1^{\infty} \frac{d\tau}{i(\nu+\kappa\tau)\sqrt{\tau^2-1}}$$

$$I_2 = -\int_1^{\infty} \frac{d\tau}{i(\nu-\kappa\tau)\sqrt{\tau^2-1}}$$

$$I_3 = -\int_1^{\infty} \frac{d\tau}{i(\nu+\kappa\tau)\sqrt{\tau^2-1}} e^{-i\kappa\tau+i(\nu+\kappa\tau)\frac{\tau+1}{\tau-1}x}$$

$$I_4 = \int_1^{\infty} \frac{d\tau}{i(\nu-\kappa\tau)\sqrt{\tau^2-1}} e^{i\kappa\tau+i(\nu-\kappa\tau)\frac{\tau-1}{\tau+1}x}$$

and $\nu = \gamma - \kappa M$. By substituting $2z + 1 = \tau$ into I_1 and I_2 they may be expressed in the following form

$$I_j = \frac{1}{2i\kappa} \int_0^\infty z^{-\frac{1}{2}}(z+1)^{-\frac{1}{2}}(z+\Omega_j)^{-1} dz \quad j = 1,2$$

where

$$\Omega_1 = \frac{\kappa + \nu}{2\kappa} \quad \text{and } \Omega_2 = \frac{\kappa - \nu}{2\kappa}$$

This integral may be found in Gradshteyn and Ryzhik (1965) to be

$$I_j = \frac{1}{i\kappa} \frac{\arcsin\sqrt{1-\Omega_j}}{\sqrt{\Omega_1 \Omega_2}}$$

Adding I_1 and I_2 we find

$$I_1 + I_2 = \frac{\pi}{i\sqrt{\kappa^2 - \nu^2}} \tag{3.14}$$

Substitution of $z = \sqrt{\frac{\tau+1}{\tau-1}}$ into the expression for I_3 and $z = \sqrt{\frac{\tau-1}{\tau+1}}$ into the expression for I_4 and the addition of the resulting equations leads to

$$I_3 + I_4 = -\frac{2}{i(\kappa+\nu)} e^{i\kappa x} \int_0^\infty \frac{e^{ix(\kappa+\nu)z^2}}{z^2 + \frac{\kappa-\nu}{\kappa+\nu}} dz$$

From Gradshteyn and Ryzhik (1965) the following solution may be obtained

$$I_3 + I_4 = -\frac{\pi}{i\sqrt{\kappa^2 - \nu^2}} e^{i\nu x} (1 - \operatorname{erf}\sqrt{-ix(\kappa - \nu)}) \tag{3.15}$$

Equations (3.13),(3.14) and (3.15) may be combined to give the pressure, $\bar{p}(x, +0)$, on the surface

$$\bar{p}(x, +0) = -\frac{\hat{P}}{i\sqrt{\kappa^2 - \nu^2}} e^{i\nu x} \operatorname{erf}\sqrt{-ix(\kappa - \nu)}$$

The pressure, $\bar{p}(x, -0)$ on the lower surface is equal to the negative of the pressure on the upper surface. If the pressure difference across the plate is defined as $\Delta\bar{p} = \bar{p}(x, -0) - \bar{p}(x, +0)$, then the load distribution on the plate is

$$\Delta p(x) = \frac{2\hat{P}}{i\sqrt{\kappa^2 - \nu^2}} e^{i\gamma x} \operatorname{erf}\sqrt{-ix(\kappa - \nu)} \tag{3.16}$$

3.2 The leading edge problem

Consider a semi-infinite plate located at $x \geq 0$, $y = 0$ with a mean flow directed in the positive x-direction. The perturbation velocity is split up in two parts; one due to the incident wave and another due to the diffracted wave. Moreover, if the velocity due to the diffracted wave is expressed in terms of a velocity potential, ϕ, the boundary value problem for the diffracted wave becomes

$$\frac{\partial^2 \bar{\phi}}{\partial x^2} + \frac{\partial^2 \bar{\phi}}{\partial \bar{y}^2} + \kappa^2 \bar{\phi} = 0 \tag{3.17}$$

$$\frac{\partial \bar{\phi}}{\partial \bar{y}} = -\frac{1}{\beta} w^{inc}(x) e^{-i\kappa M x} \quad \text{for } x > 0,\ \bar{y} = 0 \tag{3.18}$$

$$\bar{\phi} = 0 \quad \text{for } x < 0,\ \bar{y} = 0 \tag{3.19}$$

where $w^{inc}(x)$ is the normal velocity of the incident wave. Assuming that the incoming wave is a plane wave so that

$$w^{inc}(x) = \hat{w} e^{i\gamma x}$$

and using the same method as in the trailing edge problem one finds the jump in velocity potential across the plate to be

$$\Delta\phi(x) = \phi(x,-0) - \phi(x,+0) = -\frac{2\hat{w}}{i\beta\sqrt{\kappa^2 - \nu^2}} e^{i\gamma x} \mathrm{erf}\sqrt{ix(\kappa+\nu)} \tag{3.20}$$

The pressure jump across the plate is obtained by using the momentum equation

$$(i\lambda + \frac{\partial}{\partial x})\Delta\phi(x) = -\Delta p(x) \tag{3.21}$$

Substitution of eq.(3.20) into eq.(3.21) leads to the following expression for the loading on the plate

$$\Delta p(x) = \frac{2\hat{w}}{\sqrt{i(1-M^2)(\kappa-\nu)}} \{ i(\lambda+\gamma) e^{i\gamma x} \frac{\mathrm{erf}\sqrt{ix(\kappa+\nu)}}{\sqrt{i(\kappa+\nu)}} + \frac{e^{-i\frac{\lambda M}{1+M}x}}{\sqrt{\pi x}} \} \tag{3.22}$$

This is the general expression for the loading on the plate due to waves incident on the leading edge. Specifically if the incident wave is a *vorticity wave*, then $\gamma = -\lambda$ and equation (3.22) reduces to

$$\Delta p(x) = \frac{2\hat{w}}{\sqrt{\pi\lambda(1+M)x}} e^{-i(\frac{\lambda M}{1+M}x + \frac{\pi}{4})} \tag{3.23}$$

Chapter 4
Reflection Coefficients

An oscillating cascade emits upstream propagating pressure waves and downstream propagating waves; pressure waves and vorticity waves. When these waves impinge on a neigboring cascade or row of stator blades a part of the wave is reflected and another part is transmitted. It is possible that these reflected waves may give rise to a negative aerodynamic damping on the oscillating cascade. To determine this it is therefore of interest to know the reflection coefficients.

In this chapter expressions for the reflection coefficents of a cascade subjected to plane incident waves are derived. In section 4.1 the reflection coefficients are derived by modelling the cascade blades as semi-infinite flat plates. In section 4.2 the semi-actuator disk theory developed by Kaji and Okazaki (1970a) is used to obtain the reflection coefficients. A comparison between the reflection coefficients of section 4.1 and 4.2 is carried out in section 4.3.

4.1 Semi-infinite plate approximation

In this section the pressure jumps across a semi-infinte plate derived in chapter 3 are used to derive reflection coefficients. By using these pressure jumps in conjuction with equations (2.12) and (2.15) it is possible to obtain simple formulas for the reflection coefficients.

A wave incident on a cascade give rise to a number of different reflected wave modes. If we are concerned with propagating modes only, we know from the condition (2.23)

that the number is limited when the axial Mach number is less than 1. Let $R(n)$ denote the reflection coefficient for the n:th reflected pressure mode and $\hat{p}^{inc}$ the amplitude of the incident pressure wave, then the pressure due to all the reflected wave modes may be expressed as

$$p^{ref} = \sum_{nmin}^{nmax} R(n)\hat{p}^{inc} e^{i(\lambda t + \alpha_n x + \mu_n y)}$$

In the following subsections the reflection coefficients $R(n)$ are derived for the three cases; pressure wave incident on the trailing edge, pressure wave incident on the leading edge, vorticity wave incident on the leading edge. For the derivation assume that incident pressure wave is of the form:

$$p_j^{inc} = \hat{p}_j^{inc} e^{i(\lambda t + k_j x + hy)} \quad j = 1, 2 \tag{4.1}$$

where subscript 1 and 2 refers to upstream and downstream propagating waves respectively. Moreover, let the normal velocity of the incident vorticity wave be

$$w_3^{inc} = \hat{w}_3^{inc} e^{i(\lambda t + k_3 x + hy)} \tag{4.2}$$

4.1.1 Case 1: Pressure wave incident on the trailing edge

When a pressure wave is incident on the trailing edge of the cascade a pressure wave and a vorticity wave are reflected. Since the reflected pressure wave in this case is a downstream propagating wave the kernel function (2.19) is applicable. Equations (2.12) and (2.19) give the following expression for the amplitude of the n:th reflected pressure mode:

$$\hat{p}_{n2} = -\frac{\mu_n \cos\theta - \alpha_{n2} \sin\theta}{S(1 - M_x^2)(\alpha_{n2} - \alpha_{n1})} \int_{-1}^{0} e^{-i(\alpha_{n2} \cos\theta + \mu_n \sin\theta)\xi_0} \Delta p(\xi_0)\, d\xi_0 \tag{4.3}$$

The component normal to the blade of the reflected vorticity wave is given by Eq.(2.15) and the kernel function (2.22). The amplitude of n:th mode of reflected vorticity wave is found to be

$$\hat{w}_{n3} = -\frac{\lambda^2 \cos\theta}{S(\lambda^2 + \mu_n^2 + 2\lambda\mu_n \sin\theta)} \int_{-1}^{0} e^{i\lambda\xi_0} \Delta p(\xi_0)\, d\xi_0 \tag{4.4}$$

In the above equations Δp is chosen according to the trailing edge problem, i.e:

$$\Delta p = \frac{2\hat{P}}{i\sqrt{\kappa^2 - \nu_1^2}} e^{i\gamma_1\xi_0} \operatorname{erf}\sqrt{-i\xi_0(\kappa - \nu_1)}$$

where

$$\hat{P} = -\frac{i(h\cos\theta - k_1 \sin\theta)}{\beta} \hat{p}_1^{inc}$$

$$\gamma_1 = k_1 \cos\theta + h \sin\theta$$
$$\nu_1 = \gamma_1 - \kappa M$$

Substitution of Δp into the above equations (4.3) and (4.4) and integrating by parts once leads to the following reflection coefficients for the n:th modes:

$$R_I^p(n) = \frac{\hat{p}_{n2}}{\hat{p}_1^{inc}} = -\frac{2(\mu_n \cos\theta - \alpha_{n2}\sin\theta)(h\cos\theta - k_1\sin\theta)}{\beta S(1 - M_x^2)(\alpha_{n2} - \alpha_{n1})(\gamma_1 - \alpha_{n2}\cos\theta - \mu_n \sin\theta)\sqrt{i(\kappa + \nu_1)}} \times$$

$$\times \left\{ \frac{\operatorname{erf}\sqrt{i(\frac{\lambda M}{1-M} - \alpha_{n2}\cos\theta - \mu_n \sin\theta)}}{\sqrt{i(\frac{\lambda M}{1-M} - \alpha_{n2}\cos\theta - \mu_n \sin\theta)}} - e^{-i(\gamma_1 - \alpha_{n2}\cos\theta - \mu_n \sin\theta)} \frac{\operatorname{erf}\sqrt{i(\kappa - \nu_1)}}{\sqrt{i(\kappa - \nu_1)}} \right\} \tag{4.5}$$

and

$$R_I^w(n) = \frac{\hat{w}_{n3}}{\hat{w}_1^{inc}} = -\frac{2\lambda^2 \cos\theta}{S(\lambda^2 + \mu_n^2 + 2\lambda\mu_n \sin\theta)\sqrt{i(\kappa + \nu_1)}\sqrt{1 - M^2}} \times$$

$$\times \left\{ \frac{\operatorname{erf}\sqrt{i\frac{\lambda}{1-M}}}{\sqrt{i\frac{\lambda}{1-M}}} - e^{-i(\lambda+\gamma)} \frac{\operatorname{erf}\sqrt{i(\kappa - \nu_1)}}{\sqrt{i(\kappa - \nu_1)}} \right\} \tag{4.6}$$

where $\hat{w}_1^{inc}$ is the amplitude of the normal velocity associated with the incident pressure wave.

4.1.2 Case 2: Pressure wave incident on the leading edge

When a pressure wave impinges on the leading edge an upstream propagating pressure wave is reflected. It is obtained from equations (2.12) and (2.17) so the n:th mode of the

reflected wave is

$$\hat{p}_{n1} = -\frac{\mu_n \cos\theta - \alpha_{n1}\sin\theta}{S(1-M_x^2)(\alpha_{n2}-\alpha_{n1})}\int_{-1}^{0} e^{-i(\alpha_{n1}\cos\theta+\mu_n\sin\theta)\xi_0}\Delta p(\xi_0)\,d\xi_0 \tag{4.7}$$

In this case the pressure jump from the leading edge problem, eq (3.22), is used, i.e.,

$$\Delta p = \frac{2\hat{w}_2^{inc}}{i\beta\sqrt{\kappa^2-\nu_2^2}}\{\frac{\sqrt{i(\kappa+\nu_2)}}{\sqrt{\pi\xi_0}}e^{-i\frac{\lambda M}{1+M}\xi_0} + i(\lambda+\gamma_2)e^{i\gamma_2\xi_0}\,\mathrm{erf}\sqrt{i\xi_0(\kappa+\nu_2)}\}$$

where

$$\gamma_2 = k_2\cos\theta + h\sin\theta$$
$$\nu_2 = \gamma_2 - \kappa M$$

From the momentum equation a relation between the amplitude of the normal velocity and the amplitude of the pressure in the incident wave may be found to be

$$\hat{w}_2^{inc} = -\frac{h\cos\theta - k_2\sin\theta}{\lambda+\gamma_2}\hat{p}_2^{inc}$$

Substituting the above expression and the expression for Δp into equation (4.7) and using integration by parts we obtain the following expression:

$$R_{II}(n) = \frac{\hat{p}_{n1}}{\hat{p}_2^{inc}} = -\frac{2(\mu_n\cos\theta - \alpha_{n1}\sin\theta)(h\cos\theta - k_2\sin\theta)}{S\beta(1-M^2\cos^2\theta)(\alpha_{n2}-\alpha_{n1})(\lambda+\gamma_2)\sqrt{i(\kappa-\nu_2)}}\times$$

$$\times\{(1-\frac{\lambda+\gamma_2}{g})\frac{\mathrm{erf}\sqrt{if}}{\sqrt{if}} + \frac{\lambda+\gamma_2}{g}e^{ig}\frac{\mathrm{erf}\sqrt{i(\kappa+\nu_2)}}{\sqrt{i(\kappa+\nu_2)}}\} \tag{4.8}$$

where

$$g = \gamma_2 - \alpha_{n1}\cos\theta - \mu_n\sin\theta$$

and

$$f = \frac{\lambda M}{1+M} + \alpha_{n1}\cos\theta + \mu_n\sin\theta$$

4.1.3 Case 3: Vorticity wave incident on the leading edge

When a vorticity wave impinges on the leading edge the reflected wave will be an upstream propagating pressure wave. The normal velocity associated with this pressure wave is given by equations (2.15) and (2.17). In conjunction with these equations the

expression for the pressure jump across a semi-infinite plate equation (3.23) is used.

$$\Delta p = \frac{2\hat{w}_3^{inc}}{\sqrt{i\pi(1+M)\lambda\xi_0}} e^{-i\frac{\lambda M}{1+M}\xi_0}$$

Substitution of Δp and equation (2.17) into equation (2.15) and straight forward integration yields

$$R_{III}(n) = \frac{\hat{w}_{n1}}{\hat{w}_3^{inc}} = \frac{(\mu_n \cos\theta - \alpha_{n1}\sin\theta)^2}{S(1-M^2\cos^2\theta)(\alpha_{n2}-\alpha_{n1})(\lambda+\alpha_{n1}\cos\theta+\mu_n\sin\theta)\sqrt{i\lambda(1+M)}} \times$$

$$\times \frac{\mathrm{erf}\sqrt{i(\frac{\lambda M}{1+M}+\alpha_{n1}\cos\theta+\mu_n\sin\theta)}}{\sqrt{i(\frac{\lambda M}{1+M}+\alpha_{n1}\cos\theta+\mu_n\sin\theta)}} \tag{4.9}$$

4.2 Semi-actuator disk theory

In the semi-actuator disk theory the cascade is modeled as a blade row with finite chord length and with infinitesimal blade spacing. The flow field is divided into three fields; the upstream field, the downstream field, and the field inside the cascade. The upstream and downstream fields are two dimensional, while the field inside the cascade is assumed to be one- dimensional. These fields are matched through the following boundary conditions:

- the mass flow is continous at the leading edge;
- the total enthalpy is conserved at the leading edge;
- the mass flow is continous at the trailing edge;
- the total enthalpy is conserved at the trailing edge;
- the flow direction at the trailing edge is in accordance with the Kutta condition.

The density, pressure and velocities are decomposed in a steady undisturbed quantity and a small unsteady perturbation. The governing equations are linearized and non-dimensionalized in the same way as in chapter 2. Hence, the perturbation quantities in

the upstream and downstream field are governed by equations (2.5), (2.6), (2.7) and (2.8). In this theory one is concerned with propagating modes only. The perturbations are assumed to be harmonic with respect to time and space, i.e. $e^{i(\lambda t+\alpha x+\mu y)}$. Substitution of this assumption into the governing equations and the requirement that the determinant has to be zero for non-trival solutions leads to the following relations between the wave numbers

$$\alpha_1 = \frac{M\cos\theta(M\mu\sin\theta + M\lambda) + \sqrt{(M\mu\sin\theta + M\lambda)^2 - (1 - M^2\cos^2\theta)^2\mu^2}}{1 - M^2\cos^2\theta} \tag{4.10}$$

$$\alpha_2 = \frac{M\cos\theta(M\mu\sin\theta + M\lambda) - \sqrt{(M\mu\sin\theta + M\lambda)^2 - (1 - M^2\cos^2\theta)^2\mu^2}}{1 - M^2\cos^2\theta} \tag{4.11}$$

$$\alpha_3 = -\frac{\lambda + \mu\sin\theta}{\cos\theta} \tag{4.12}$$

where subscript 1, 2 and 3 are the wave numbers corresponding to upstream propagating pressure wave, downstream propagating pressure wave and vorticity wave, respectively. These relations are the same as the relations between the α:s and μ:s in chapter 2. From equations (2.6) and (2.7) the relations between the amplitude of the pressure and the amplitude of the velocities are found to be

$$\hat{u}_1 = -\alpha_1 A\hat{p}_1 \tag{4.13}$$
$$\hat{v}_1 = -\mu A\hat{p}_1 \tag{4.14}$$
$$\hat{u}_2 = -\alpha_2 B\hat{p}_2 \tag{4.15}$$
$$\hat{v}_2 = -\mu B\hat{p}_2 \tag{4.16}$$
$$\alpha_3\hat{u}_3 = -\mu\hat{v}_3 \tag{4.17}$$

where

$$A = (\lambda + \alpha_1\cos\theta + \mu\sin\theta)^{-1} \tag{4.18}$$
$$B = (\lambda + \alpha_2\cos\theta + \mu\sin\theta)^{-1} \tag{4.19}$$

Inside the cascade the linearized and non-dimensionalized governing equations are

$$\frac{\partial\rho}{\partial t} + \frac{\partial\rho}{\partial x_1} + \frac{\partial u_c}{\partial x_1} = 0 \tag{4.20}$$

$$\frac{\partial u_c}{\partial t} + \frac{\partial u_c}{\partial x_1} = -\frac{\partial p}{\partial x_1} \tag{4.21}$$

where u_c denotes the streamwise velocity inside the cascade. The perturbations inside the cascade are assumed to be harmonic functions of time and space, i.e. $e^{i(\lambda t+\gamma x_1)}$. Moreover, one assumes that there is no vorticity wave in the cascade. An analogous procedure to that for the upstream and downstream field leads the following relations between the wave numbers and the frequency:

$$\gamma_1 = \frac{\lambda M}{1-M}, \quad \gamma_2 = -\frac{\lambda M}{1+M} \tag{4.22}$$

where γ_1 and γ_2 are the streamwise wave numbers for the upstream and downstream propagating waves inside the cascade, respectively. From equation (4.21) the following relations are found:

$$\hat{u}_{c1} = -M\hat{p}_{c1} \tag{4.23}$$

$$\hat{u}_{c2} = M\hat{p}_{c2} \tag{4.24}$$

When the fields are matched the pressure waves in the cascade are expressed in the form $e^{i(\lambda t+\gamma_j x_1+\mu y)}$ $(j = 1, 2)$, with the phase factor $e^{i\mu y}$. The motivation for this is that the phase change of the wave motion in the cascade direction must coincide with that in the upstream or downstream flow.

The matching conditions are when expressed in non-dimensional form as follows: Conservation of mass at the leading edge

$$u_u + \rho_u \cos\theta = (u_c + \rho_c)\cos\theta \tag{4.25}$$

Conservation of total enthalpy at the leading edge

$$p_u + u_u \cos\theta + v_u \sin\theta = p_c + u_c \tag{4.26}$$

At the trailing edge, conservation of mass and total ethalpy, and the Kutta condition gives

$$u_c \cos\theta = u_d \tag{4.27}$$

$$u_c \sin\theta = v_d \tag{4.28}$$

$$p_c = p_d \tag{4.29}$$

where subscript u, c and d refers to the upstream field, the field within the cascade and the downstream field respectively.

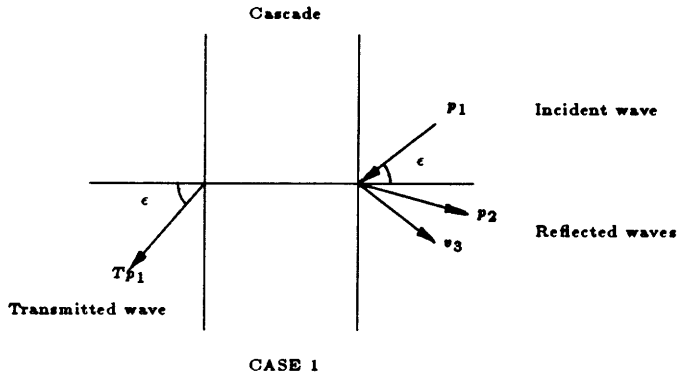

Figure 4.1: Wave reflection by the cascade; Case 1

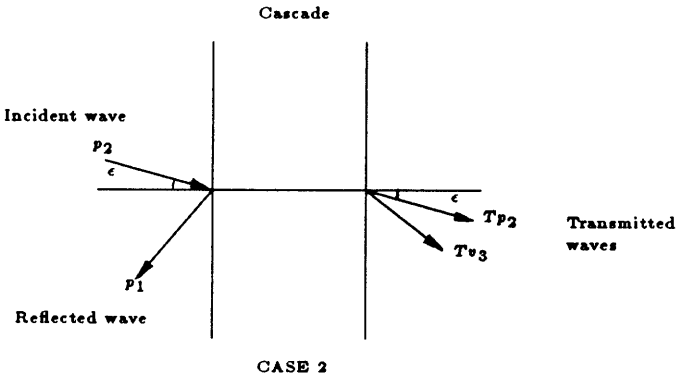

Figure 4.2: Wave reflection by the cascade; Case 2

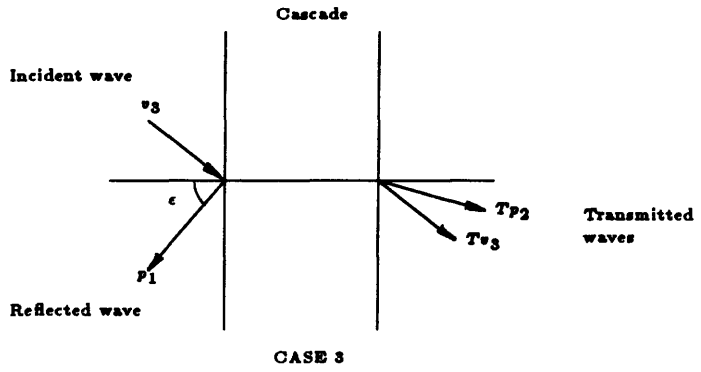

Figure 4.3: Wave reflection by the cascade; Case 3

4.2.1 Case 1: Pressure wave incident on the trailing edge

If a pressure wave hits the cascade at the trailing edge, then a pressure wave and a vorticity wave is reflected, and a pressure wave is transmitted (see figure 4.1).

The matching conditions at the leading edge and the amplitude relations (4.13), (4.14), (4.23) and (4.24) yields

$$\hat{p}_{c1} = F\hat{p}_{c2} \tag{4.30}$$

where

$$F = -\frac{1+M}{1-M}\{\frac{M^2\cos\theta - \alpha_1 A - \lambda AM\cos\theta}{M^2\cos\theta - \alpha_1 A + \lambda AM\cos\theta}\}e^{-i(\gamma_2-\gamma_1)} \tag{4.31}$$

The matching conditions at the trailing edge and amplitude relations (4.13) through (4.17), (4.23), (4.24) and (4.30) can be combined to give the reflection coefficients R_I^p and R_I^v.

$$R_I^p = \frac{\hat{p}^{ref}}{\hat{p}^{inc}} = -\frac{\lambda M(1-F) - A(\lambda\alpha_3 + \mu^2)(1+F)}{\lambda M(1-F) - B(\lambda\alpha_3 + \mu^2)(1+F)} \tag{4.32}$$

$$R_I^v = \frac{\hat{v}_3}{\hat{v}^{inc}} = -\frac{\alpha_3}{\lambda\mu A}\{\, B(\alpha_2\sin\theta - \mu\cos\theta)R_I^p + A(\alpha_1\sin\theta - \mu\cos\theta)\,\} \tag{4.33}$$

4.2.2 Case 2: Pressure wave incident on the leading edge

When a pressure wave hits the cascade at the leading edge a pressure wave is reflected, and a pressure wave and a vorticity wave are transmitted (see figure 4.2). Combining the matching conditions at the trailing edge and the amplitude relations (4.15), (4.16), (4.23) and (4.24) gives

$$\hat{p}_{c1} = F_2 \hat{p}_{c2} \tag{4.34}$$

$$F_2 = \frac{\lambda M - B(\alpha_2\alpha_3 + \mu^2)}{\lambda M + B(\alpha_2\alpha_3 + \mu^2)} e^{i(\gamma_2 - \gamma_1)} \tag{4.35}$$

The matching conditions at the leading edge and the amplitude relations (4.13) through (4.17), (4.23), (4.24) and (4.34) gives the reflection coefficient R^p_{II}

$$R_{II} = \frac{\hat{p}^{ref}}{\hat{p}^{inc}} =$$

$$= -\frac{\lambda M\{1 + M - F_2(1 - M)\}B\cos\theta - \{1 + M + F_2(1 - M)\}(M^2\cos\theta - \alpha_2 B)}{\lambda M\{1 + M - F_2(1 - M)\}A\cos\theta - \{1 + M + F_2(1 - M)\}(M^2\cos\theta - \alpha_1 A)} \tag{4.36}$$

4.2.3 Case 3: Vorticity wave incident on the leading edge

When a vorticity wave hits the cascade at the leading edge a pressure wave is reflected, and a pressure wave and a vorticity wave are transmitted (see figure 4.3). In this case the amplitude relations are the same as in case 2. Combination of the matching conditions and the amplitude relations at the trailing edge leads to the same relation between $\hat{p}_{c1}$ and $\hat{p}_{c2}$ as in case 2. The remaining matching conditions can be combined to get the reflection coefficient R_{III}

$$R_{III} = \frac{\hat{v}^{ref}}{\hat{v}^{inc}} =$$

$$= \frac{M\{1 + M - F_2(1 - M)\}(\alpha_3\sin\theta - \mu\cos\theta)\cos\theta + \{1 + M + F_2(1 - M)\}\mu}{\lambda M\{1 + M - F_2(1 - M)\}A\cos\theta - \{1 + M + F_2(1 - M)\}(M^2\cos\theta - \alpha_1 A)} \frac{\mu A}{\alpha_3} \tag{4.37}$$

4.3 Comparison between the theories

In this section a comparison is carried out between the reflection coefficients obtained by semi-actuator disk theory (SAD theory) and the reflection coefficient for the zeroth mode obtained by approximating the blades as semi-infinite plates. The reason for this choice is that the SAD theory can only predict one reflected wave which corresponds to the zeroth mode in the semi-infinite plate (SIP) approximation.

The following figures 4.4- 4.9 are plots of the absolute value of the reflection coefficients versus angle of incidence. In these plots the symbols is the result according to SAD theory and the solid lines is the result obtained by the SIP approximation. All plots are done for the same Mach number, $M = 0.5$, and the same angle of stagger, $\theta = 60°$.

In case 1 (see figures 4.4 and 4.5) the SIP approximation is in close agreement with the SAD theory in the portion between the zeroes, i.e $\epsilon = -38° - 60°$, for both frequencies. That the agreement is so good even for the low frequency is surprising. Since the SIP approximation neglects the interference between the blades in the cascade one expect it to be a good approximation for high frequencies only. For large negative angles the agreement is bad the main reason for this is that it is not a trailing edge problem any more, that is the pressure wave no longer impinges on the trailing edge but comes from a location ahead of the trailing edge and leaves it.

In case 2 (see figures 4.6 and 4.7) the SIP approximation is poor for the lower frequency but the qualitatively behavior is correct. The reason for the poor agreement is the negligence of interference betweeen blades in combination with the fact that the Kutta condition is not satisfied. For the higher frequency the agreement has improved.

In case 3 the agreement is close between SIP approximation and the SAD theory for positive angles of incidence. For negative angles of incidence the agreement improves with increasing frequency.

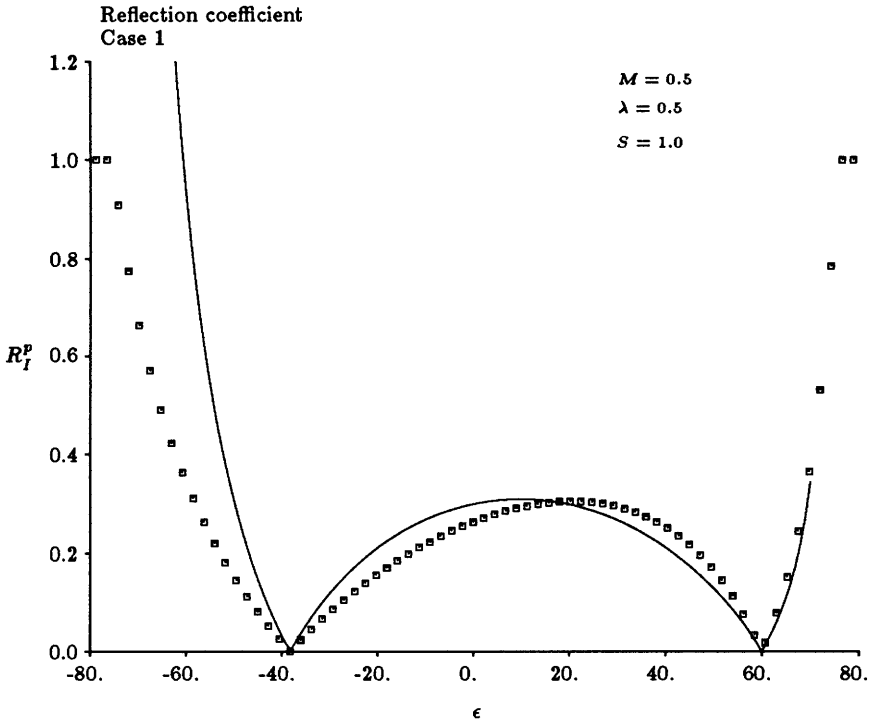

Figure 4.4: $\left| \frac{p^{ref}}{p^{inc}} \right|$ versus angle of incidence.

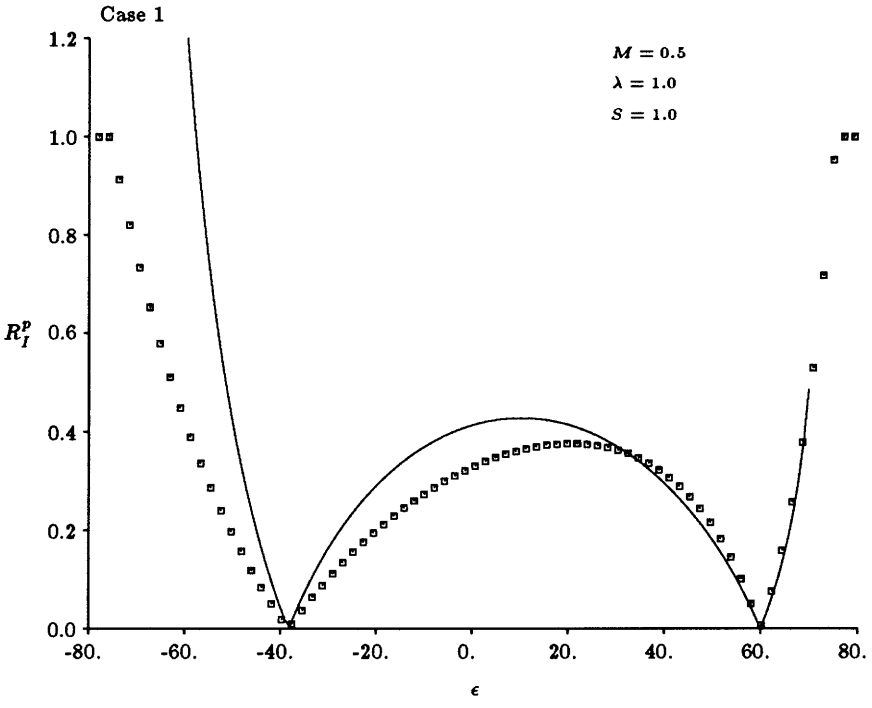

Figure 4.5: $\left| \frac{p^{ref}}{p^{inc}} \right|$ versus angle of incidence.

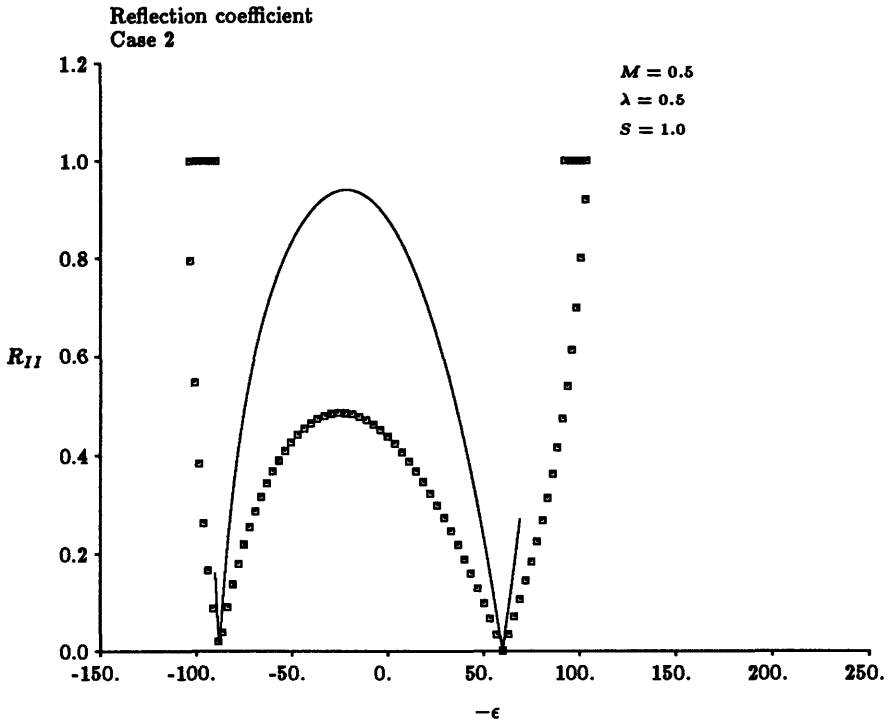

Figure 4.6: $\left| \frac{p^{ref}}{p^{inc}} \right|$ versus angle of incidence.

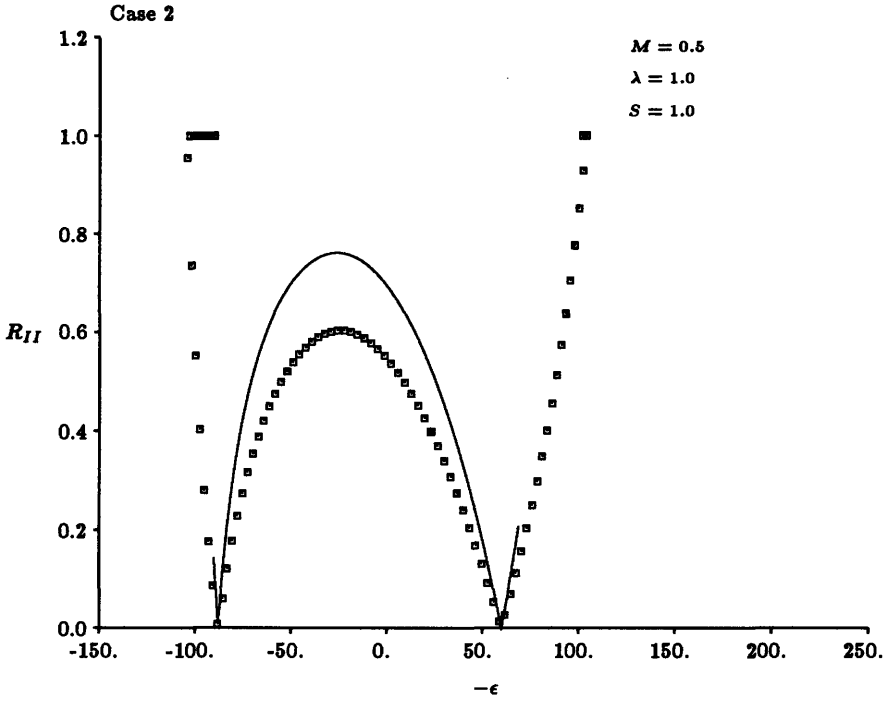

Figure 4.7: $\left| \frac{p^{ref}}{p^{inc}} \right|$ versus angle of incidence.

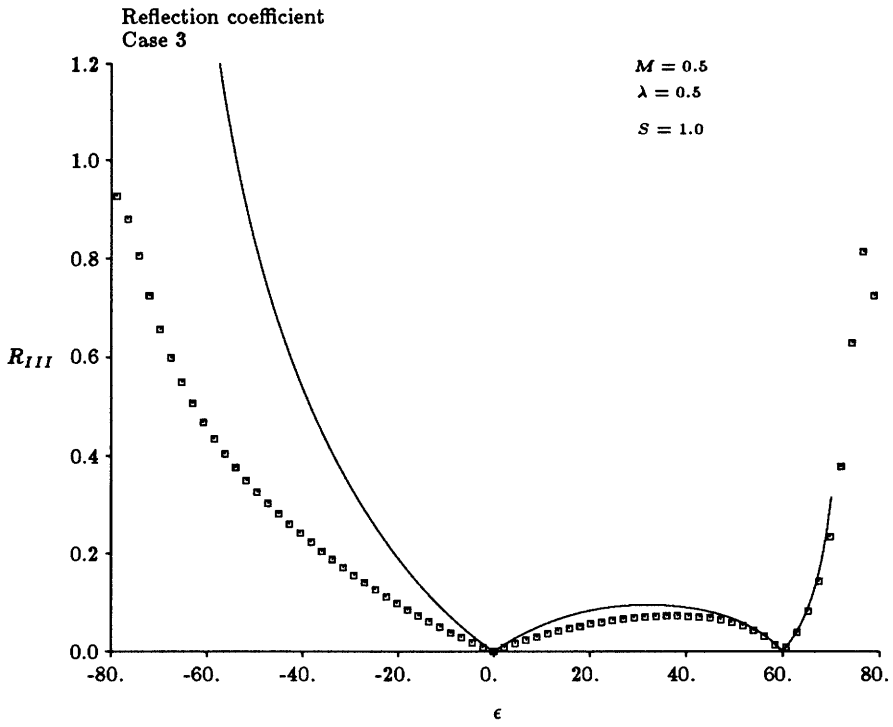

Figure 4.8: $\left| \frac{v^{ref}}{v^{inc}} \right|$ versus angle of incidence.

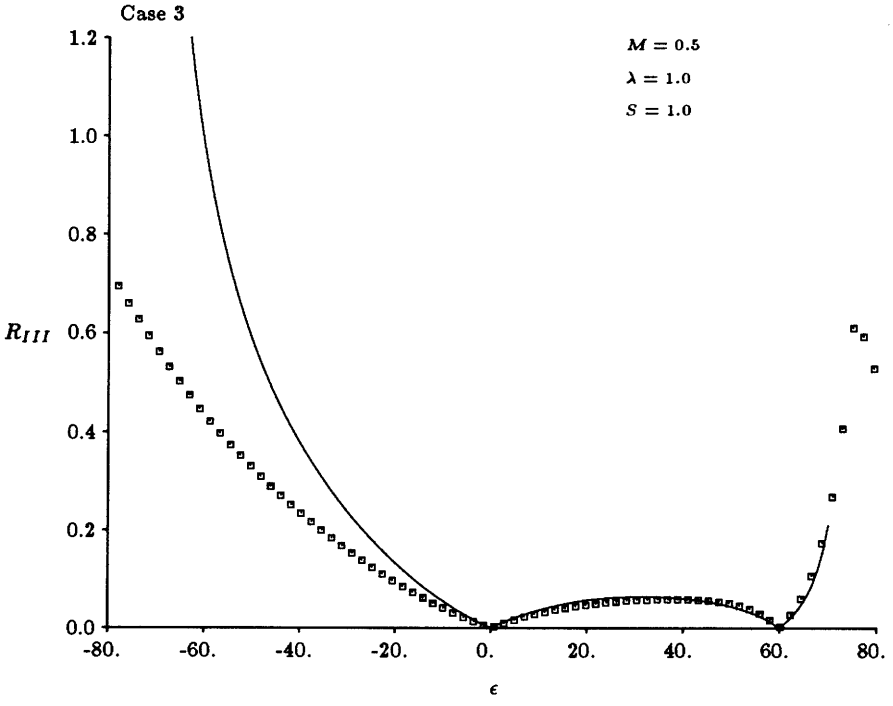

Figure 4.9: $\left| \frac{v^{ref}}{v^{inc}} \right|$ versus angle of incidence.

Chapter 5
Examples of application for the reflection coefficients

In this chapter examples of application involving reflection coefficients are shown. Section 5.1 outlines a model for stator rotor interaction based on the models in chapter 2 and section 4.1, respectively. In section 5.2 the use of reflection coefficients to modify the boundary condition in a computer code is outlined.

5.1 Stator-rotor interaction

Consider an oscillating rotor blade row and upstream of it a row of stationary blade. The vibrating blade row emits pressure waves. These waves are partially reflected back to the rotor and changes the conditions for it. By modelling reflection at the stator with the result from section 4.1 and the rotor as flat plate cascade it is possible to formulate an integral equation for zeroth rotor blade which includes effects due to the stator. From this integral equation the pressure loading on the rotor blade may be solved for when the motion of the rotor blade is prescribed.

The rotor is assumed to have the nondimensional tangential velocity V and the rotor and stator are assumed to be lightly loaded. This implies that the angle of attack is small. Let the angle of stagger of the stator be θ_s (see figure 5.1). Moreover, let S_s and c_s denote the blade spacing and the chord length respectively. The lengths used in this formulation are non- dimensionalized by the rotor chord length and the velocities by the velocity relative to the rotor.

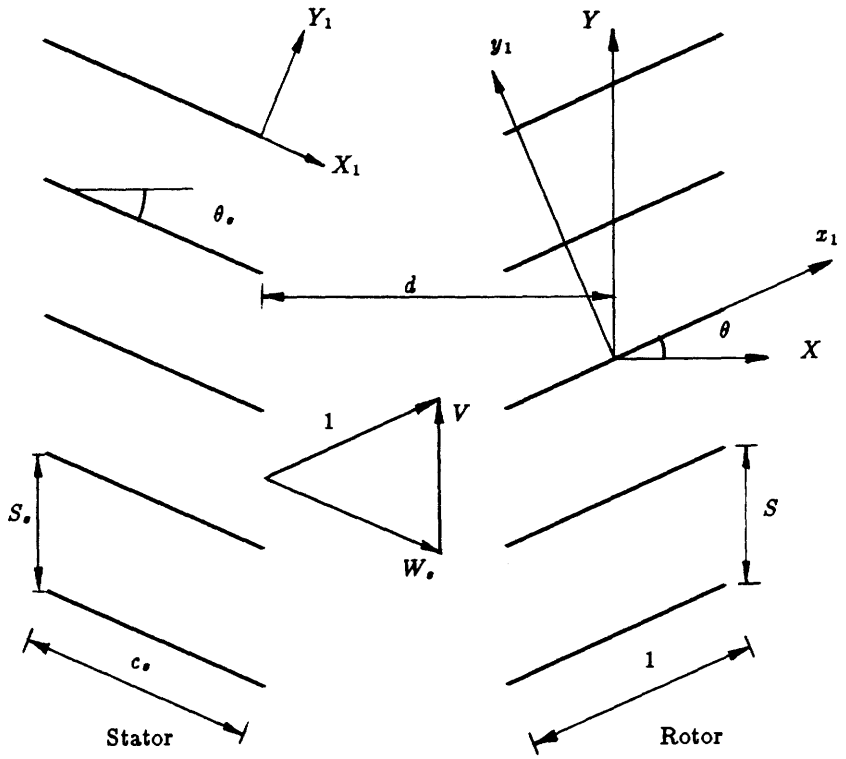

Figure 5.1: Configurations of cascades and coordinate systems

Consider the propagating modes of the emitted waves. They are of the form

$$p_{j1} = \hat{p}_{j1} e^{i(\lambda t + \alpha_{j1} x + \mu_j y)} \tag{5.1}$$

where subscript 1 is used to emphasize that the wave is an upstream propagating wave and j is the mode number. The amplitudes of these waves are given by equations (2.12) and (2.17) with $x_1 = y_1 = 0$. To calculate the reflection and be able to use the expressions in section 4.1 a transformation to a space fixed coordinate system (X, Y) is necessary. This transfomation is given by

$$x = X \quad y = Y + Vt \tag{5.2}$$

When transforming to a space fixed coordinate system the wave number remains the same but the frequency, λ_{SF}, felt in this coordinate system is different. Where this frequency is found by substituting the coordinate transformation into expression for the wave (5.1):

$$\lambda_{SF} = \lambda + V\mu_j$$

The amplitudes of the reflected pressure waves may be obtained from eq.(4.5) but it has to be modified, since the equations in section 4.1 are non-dimensionalized with the chord lenght of and the velocity relative to the cascade at which the reflection take place. Let q denote the mode numbers for the propagating waves reflected from the stator. If the time and the coordinates used in the waves emitted from the rotor are rescaled with the stator chord length and the velocity relative to the stator, then the frequency and the wave numbers of the incident wave to be used in eq.(4.5) are: $\frac{c_s \lambda_{SF}}{W_s}$, $c_s \alpha_{j1}$ and $c_s \mu_j$ respectively, where W_s is the non-dimensional velocity relative to the stator. Then the rescaling of the wave numbers of the reflected waves with the rotor chord length leads to the following reflection coefficient from the upstream cascade:

$$R_I^p(q,j) = \frac{-2c_s(\mu_q \cos(-\theta_s) - \alpha_{q2}\sin(-\theta_s))(\mu_j \cos(-\theta_s) - \alpha_{j1}\sin(-\theta_s))}{i\beta_s S_s (1 - M_x^2)(\alpha_{q2} - \alpha_{q1})(\gamma_1 - \alpha_{q2}\cos(-\theta_s) - \mu_q \sin(-\theta_s))\sqrt{ic_s(\kappa_s + \nu_1)}} \times$$

$$\times \{\frac{\mathrm{erf}\sqrt{ic_s f_1}}{\sqrt{ic_s f_1}} - e^{-ic_1(\gamma_1 - \alpha_{q2}\cos(-\theta_s) - \mu_q \sin(-\theta_s))} \frac{\mathrm{erf}\sqrt{ic_s(\kappa_s - \nu_1)}}{\sqrt{ic_s(\kappa_s - \nu_1)}}\} \tag{5.3}$$

where

$$f_1 = \frac{\lambda_{SF} M_s}{W_s(1 - M_s)} - \alpha_{q2}\cos(-\theta_s) - \mu_q \sin(-\theta_s)$$

$$\kappa_s = \frac{\lambda_{SF} M_s}{W_s \beta_s}$$

$$\beta_s = 1 - M_s$$
$$\gamma_1 = \alpha_{j1}\cos(-\theta_s) + \mu_j \sin(-\theta_s)$$
$$\nu_1 = \gamma_1 - \kappa_s M_s$$

and M_s is the Mach number in the stator fixed coordinate system. The angle $-\theta_s$ is motivated by the fact that the θ:s appering in the equations of section 4.1 are defined positive in the counter clockwise direction while θ_s is defined positive clockwise. In the above equations the wave numbers of the reflected waves are given by the following equations;

$$\mu_q = \frac{2\pi q + \sigma_1}{S_s}$$

$$\alpha_{q2} = \frac{1}{\beta_x^2}\{M_x(M_s \sin(-\theta)\mu_q + \frac{\lambda_{SF}}{W_s}M_s) - \sqrt{(M_s \sin(-\theta_s)\mu_q + \frac{\lambda_{SF}}{W_s}M_s)^2 - \beta_x^2 \mu_q^2}\}$$

In a similar fashion all the other reflection coefficients may be modified.

The reflected pressure waves from the stator due to the pressure waves emitted from the rotor may by use of the above equations be expressed as

$$p_{q2} = R_I^p(q,j)\hat{p}_{j1} e^{i(\lambda_{SF} t + \alpha_{q2} X + \mu_q Y + \Psi_2)} \tag{5.4}$$

where $\Psi_2 = (\alpha_{q2} - \alpha_{j1})d$ and d is distance from midchord of the rotor baldes to the trailing edge of the stator blades. The transformation to the rotor fixed coordinate system; (x_1, y_1) (see figure 2.1) and differentiation with respect to y_1 leads to the following expression for the velocity normal to the zeroth rotor blade

$$w_{q2,NR} = w_{q2}(x_1, 0)e^{i\lambda_q t} =$$

$$= \frac{\mu_q \cos\theta - \alpha_{q2}\sin\theta}{\lambda_{(q)} + \alpha_{q2}\cos\theta + \mu_q \sin\theta} R_I^p(q,j)\hat{p}_{j1} e^{i(\lambda_q t + (\alpha_{q2}\cos\theta + \mu_q \sin\theta)x_1 + \Psi_2)} \tag{5.5}$$

where

$$\lambda_q = \lambda + V\mu_j - V\mu_q$$

The inter blade phase angle σ_s for the stator is related to the wave number μ_j through

$$\sigma_s = \mu_j S_s$$

Moreover, since $\mu_q = \frac{2\pi q + \sigma_s}{S_s}$, λ_q may be expressed as

$$\lambda_q = \lambda - \frac{2\pi q}{S_s} \tag{5.6}$$

On impingement with the upstream blade row the upstream propagating pressure wave, p_{j1}, produces a downstream travelling vorticity wave. To obtain an expression for the amplitude of this vorticity wave from eq. (4.6) the velocity component normal to the stator blade surface of associated with p_{j1} is needed. Let the (X_1, Y_1)-system be a coordinate system fixed to the stator such that X_1 is parallell to the blade surfaces and Y_1 normal to the blades then they are related to (X, Y) through

$$\begin{aligned} X &= X_1 \cos\theta_s + Y_1 \sin\theta_s - d \\ Y &= -X_1 \sin\theta_s + Y_1 \cos\theta_s \end{aligned}$$

These relations in conjunction with the momentum equation:

$$(\frac{\partial}{\partial t} + \frac{\cos\theta}{\cos\theta_s}\frac{\partial}{\partial X_1})w_{j1,NS} = -\frac{\partial}{\partial Y_1}p_{j1}$$

leads to

$$\hat{w}_{j1,NS} = -\frac{\alpha_{j1}\sin\theta_s + \mu_j\cos\theta_s}{\lambda_{SF} + \alpha_{j1}\cos\theta - \mu_j\cos\theta\tan\theta_s}\hat{p}_{j1} \tag{5.7}$$

where subscript NS is used to emphasize that the velocity is normal to the stator blades. If the reflection coefficient R_I^w of section 4.1 is modified in the same way as R_I^p above, then the q:th mode of the produced vorticity wave can be expressed as

$$w_{q3,NS} = -\frac{\alpha_{j1}\sin\theta_s + \mu_j\cos\theta_s}{\lambda_{SF} + \alpha_{j1}\cos\theta - \mu_j\cos\theta\tan\theta_s}R_I^w(q,j)\hat{p}_{j1}e^{i(\lambda_{SF}t + \alpha_{q3}X + \mu_q Y + \Psi_3)} \tag{5.8}$$

where $\Psi_3 = (\alpha_{q3} - \alpha_{j1})d$. The property that the vorticity is divergence free and the relation between (X_1, Y_1) and the coordinate system (x_1, y_1) with axis parallel and normal to the rotor blades leads to

$$w_{q3,NR} = -\frac{(\alpha_{j1}\sin\theta_s + \mu_j\cos\theta_s)(\lambda_{SF}\cos\theta - \mu_q\sin(\theta+\theta_s))}{\lambda_{SF}\cos\theta_s(\lambda_{SF} + \alpha_{j1}\cos\theta - \mu_j\cos\theta\tan\theta_s)}\times$$

$$\times R_I^w(q,j)\hat{p}_{j1}e^{i(\lambda_q t+(\alpha_{q3}\cos\theta+\mu_q\sin\theta)x_1+\Psi_3)} = w_{q3}(x_1,0)e^{i\lambda_q t} \tag{5.9}$$

where
$$R_I^w(q,j) = -\frac{2c_s(\frac{\lambda_{SF}}{W_s})^2\cos(-\theta_s)}{S_s\{(\frac{\lambda_{SF}}{W_s})^2+\mu_q^2+2(\frac{\lambda_{SF}}{W_s})\mu_q\sin(-\theta_s)\}\sqrt{ic_s(\kappa_s+\nu_s)}\sqrt{1-M_s^2}}\times$$

$$\times\{\frac{\mathrm{erf}\sqrt{ic_s\frac{\lambda_{SF}}{W_s(1-M)}}}{\sqrt{i\frac{\lambda_{SF}}{W_s(1-M)}}} - e^{-ic_s(\frac{\lambda_{SF}}{W_s}+\gamma)}\frac{\mathrm{erf}\sqrt{ic_s(\kappa_s-\nu_s)}}{\sqrt{ic_s(\kappa_s-\nu_s)}}\} \tag{5.10}$$

and
$$\alpha_{q3} = -\frac{\frac{\lambda_{SF}}{W_s c_s}+\mu_q\sin(-\theta_s)}{\cos(-\theta_s)}$$

It is natural to expand a prescribed motion of the blade in a Fourier series in time of the fundamental frequency;
$$\lambda_0 = \frac{2\pi V}{S_s}$$
By doing this it is possible to express the total upwash on the blade for each harmonic component. Let $w^m_{pres}(x_1,y_1)$ be the velocity amplitude of the m:th harmonic of the prescribed motion then the boundary condition of no flow through the blade gives:

$$w^m_{pres}(x_1,0) = w^m(x_1,0) + \sum_j\sum_l\{w_{(l-m)2}(x_1,0) + w_{(l-m)3}(x_1,0)\}$$

where w^m is given by equations (2.15),(2.18) and(2.20). $w_{(l-m)2}$ and $w_{(l-m)3}$ are given by equations (5.5) and (5.9), respectively. All terms on the right hand side depend on the pressure jump across the blade, which has to be solved for numerically.

5.2 Reflection coefficients as boundary condition

The reflection coefficients may be implemented in a computer code to modify the boundary conditions to include reflection in neighboring blade rows. How this can be done depends on what type of code one wants to implement them in. Commonly one uses absorbing boundary conditons in computer codes, i.e the outgoing waves propagates out

of the computational domain without reflection in the boundaries of the computational domain. That is to say that the incoming pressure waves, vorticity waves and entropy waves are all zero. By including reflection in the relations for the total perturbation quantities (sum of the outgoing and the reflected parts) at the boundaries it is possible to include effects that may arise from this phenomenon. Reflection may give rise to standing wave patterns between rotor and stator. How this phenomenon affect the aeroelastic behavior of the rotor is still not known. Wave reflection also give rise to fluctuating forces on the cascade blade which may affect the aerodynamic damping for the blade.

As was pointed out in the previous section the reflection coefficients of section 5.1 have to be modified somewhat when waves radiated from a moving cascade are reflected by a cascade at rest. If in a computer model one considers an oscillating rotor blade then the required modification of the reflection coefficients is analogous to the one carried out in the previous section. This interaction between a moving cascade and a cascade at rest is the reason for the frequency shift of the higher modes of the reflected waves. Let λ be the frequency of the outgoing wave and q the mode number then the frequencies of the reflected wave modes may be expressed as:

$$\lambda_q = \lambda - \frac{2\pi V}{S} q$$

where V is the tangential velocity of the rotor and S is the blade spacing of the stator.

At the upstream boundary

The total perturbation pressure at the upstream boundary consists of two parts. One part is due to the outgoing wave and the other part is a wave train of reflected waves. By the use of reflection coefficients the total pressue perturbation may be expressed in terms of the amplitude of the outgoing wave $\hat{p}_{out,1}$ as

$$p = \{e^{i(\lambda t + k_1 x + hy)} + \sum_q R_I^p(q) e^{i\lambda_q t + i\alpha_{q2} x + i\mu_q y}\}\hat{p}_{out,1} \tag{5.11}$$

The velocity perturbations consist of three parts. One due to the outgoing pressure wave, a wave train of reflected pressure waves and a wave train of reflected vorticity waves.

Specifically for the axial velocity perturbation this may be expressed as

$$u = \hat{u}_{out,1} e^{i(\lambda t + k_1 x + hy)} + \{\sum_q A_1(q) R_I^p(q) e^{i\lambda_q t + i\alpha_{q2} x + i\mu_q y} +$$

$$+ \sum_q B_1(q) R_I^w(q) e^{i\lambda_q t + i\alpha_{q3} x + i\mu_q y}\} \hat{p}_{out,1} \tag{5.12}$$

where A_1 and B_1 are dependent on the frequency, the wave numbers and the angle of stagger of the upstream stator blade row. A similar expression may be written for the velocity perturbation in the y-direction.

At the downsteam boundary

At the downstream boundary the perturbation pressure consists of three parts. One is due to the outgoing pressure wave, the second is a wave train due to reflection of the outgoing pressure wave and the third is a wave train due to reflection of outgoing vorticity waves.

$$p = \{e^{i(\lambda t + k_2 x + hy)} + \sum_q R_{II}(q) e^{i(\lambda - \frac{2\pi V}{S} q)t + i\alpha_{q1} x + i\mu_q y}\} \hat{p}_{out,2} +$$

$$+ \sum_q C(q) R_{III}(q) e^{i\lambda_q t + i\alpha_{q1} x + i\mu_q y} \hat{v}_{out,3} \tag{5.13}$$

where C is dependent on the frequency, the wave numbers and the angle of stagger of the downstream stator. The velocity perturbation in the x-direction may be expressed as the sum of four part: an outgoing pressure wave, an outgoing vorticity wave, a reflected part due to the outgoing pressure wave and a reflected part due to the outgoing vorticity wave.

$$u = \hat{u}_{out,2} e^{i(\lambda t + k_2 x + hy)} + \hat{u}_{out,3} e^{i(\lambda t + k_3 x + hy)} +$$

$$+ \sum_q A_2(q) R_{II}(q) e^{i\lambda_q t + i\alpha_{q1} x + i\mu_q y} \hat{p}_{out,2} +$$

$$+\sum_{q} B_2(q) R_{III}(q) e^{i\lambda_q t + i\alpha_{q1} x + i\mu_q y} \hat{v}_{out,3} \tag{5.14}$$

where A_2 and B_2 are parameters dependent on the frequency and the wave numbers. A similar expression may be written for the tangential velocity perturbation.

In the above equations the non-reflecting boundary conditions are recovered by setting all the reflection coefficients equal to zero.

Chapter 6
Conclusions

Approximate expressions for the reflection coefficients for a flat plate cascade have been derived, by modelling the blades as semi-infinite plates (SIP approximation). The agreement between these and the reflection coefficients obtained by using the semi-actuator disk theory (SAD theory) have been found to be good for high frequencies. For low frequencies only those reflection coefficients for reflection at the trailing edge are in good agreement with the SAD theory. The advantage that one has gained with the SIP approximation is that one has simple formulas for the reflection coefficients. These are expressed in terms of the frequency and the wave numbers and no numerical solution is necessary. Moreover, they can be used to predict reflection in both sub- and superresonant cases, whereas the SAD theory can handle subresonant cases only. The more accurate approach of solving the upwash integral numerically and use the obtained loading in equations (2.12) and (2.15) to calculate the reflected field takes approximately 1 minute on a computer for each incident wave. This might not seem like a long time, but in a compressor there are a large number of waves of different frequencies. Therefore, the trade off between accuracy and computational time that SIP approximation offers can be particularily attractive when there is a question of implementation in advanced computer codes.

REFERENCES

Gradshteyn, I. S., and Ryzhik, I. M. 1965. *Tables of Integrals, Series and Products.* Academic Press, New York.

Kaji, S., and Okazaki, T. 1970a. Propagation of sound waves through a blade row I. Analysis based on semi-actuator disk theory. *J. Sound Vib.*, **11**, 339-353.

Kaji, S., and Okazaki, T. 1970b. Propagation of sound waves through a blade row II. Analysis based on acceleration potential method. *J. Sound Vib.*, **11**, 355-375.

Landahl, M. T. 1961. *Unsteady Transonic Flow*, Pergamon Press, (Reprinted 1989 by Cambridge University Press, Cambridge Science Classics).

Ni, R. H. 1979. A Rational Analysis of Periodic Flow Perturbation in Supersonic Two-Dimensional Cascade. *J. Eng. Power*, **101**, 431-439.

Sidén, G. L. D. 1990. *Unsteady Navier-Stokes Solver for the Simulation of Compressor Flutter in Turbomachines*, Tekn. lic. thesis, The Department of Turbomachinery, Chalmers University of Technology, Göteborg, Sweden.

Smith, S. N. 1971. *Discrete Frequency Sound Generation in Axial Flow Turbomachines*, University of Cambridge, Department of Engineering Report CUED/A-Turbo/TR 29.

Whitehead, D. S. 1962. Force and Moment Coefficients for Vibrating Airfoils in Cascades. Aeronautical Research Council Reports and Memoranda, R & M No. 3254, Her Majesty's Stationery Office, London.

Appendix A

Derivation of the kernel functions

In this appendix a derivation of the Kernel functions K_p and K_w will be presented. The derivation follows that given by Kaji and Okazaki (1970b).

The starting point for this derivation is the following expressions for the kernel functions:

$$K_p(x_1, y_1, \xi) = \sum_{m=-\infty}^{\infty} \frac{\partial G}{\partial \eta}(x_1, y_1, \xi_m, \eta_m) e^{i\sigma m} \tag{A.1}$$

$$K_w(x_1, y_1, \xi) = -e^{-i\lambda x_1} \int_{-\infty}^{x_1} \sum_{m=-\infty}^{\infty} \frac{\partial^2 G_m}{\partial y_1 \partial \eta} e^{i\lambda x_1' + i\sigma m}\, dx_1' \ . \tag{A.2}$$

To manipulate K_w use the identity

$$\frac{\partial G}{\partial \eta} = -\frac{\partial G}{\partial y_1}$$

and that

$$\frac{\partial^2 G}{\partial y_1^2} = -\frac{i\beta}{4} e^{i\kappa M(x_1 - \xi)} \left(\frac{\partial^2}{\partial x_1^2} + \kappa^2\right) H_0^{(2)}(\kappa r)$$

Substitute these in the integral for K_w and integrate by parts twice this results in the following equation

$$K_w = \frac{i}{4\beta} \sum_{-\infty}^{\infty} e^{i\kappa M(x_1 - \xi) + i\sigma m} \left(-\beta^2 \frac{\partial}{\partial x_1} + i\lambda\right) H_0^{(2)}(\kappa r_m) +$$

$$+ \frac{i\lambda^2}{4\beta} \sum_{-\infty}^{\infty} e^{-i\lambda(x_1 - \xi) + i\sigma m} \int_{-\infty}^{x_1} e^{i\frac{\lambda}{\beta^2}(x_1' - \xi)} H_0^{(2)}(\kappa r_m)\, dx_1' \tag{A.3}$$

Since the angel of stagger is θ and the blade spacing S, the coordinates ξ_m and η_m are

$$\xi_m = \xi + mS\sin\theta \quad \text{and} \quad \eta_m = mS\cos\theta$$

Substitute these in the equations for K_p and K_w. Then introducing new independent variables q and ς defined by;

$$q = -\frac{1}{\beta_x^2}\{(x_1 - \xi)\sin\theta + \beta^2 y_1\cos\theta\}$$

$$\varsigma = \frac{\beta}{\beta_x^2} \mid (x_1 - \xi)\cos\theta - y_1\sin\theta \mid$$

we find the following equations

$$K_p = \frac{i\kappa\beta}{4} e^{i\kappa M(x_1-\xi)-iq\delta}\{(y_1 + q\cos\theta)\Sigma_1 - \cos\theta\Sigma_2\} \tag{A.4}$$

and

$$K_w = \frac{i\lambda}{4\beta} e^{i\kappa M(x_1-\xi)-iq\delta}\{M(x_1 - \xi + q\sin\theta)\Sigma_1 - M\sin\theta\Sigma_2 + i\Sigma_3\}+$$

$$+ \frac{i\lambda^2}{4\beta} e^{-i\lambda(x_1-\xi)-iq\delta}\int_{-\infty}^{x_1} e^{\frac{i\lambda}{\beta^2}(x_1'-\xi)}\Sigma_3\, dx_1' \tag{A.5}$$

where

$$\Sigma_1 = \sum_{m=-\infty}^{\infty} \frac{H_1^{(2)}(\varpi\sqrt{(q+mS)^2+\varsigma^2})}{\beta_x\sqrt{(q+mS)^2+\varsigma^2}} e^{i(q+mS)\delta} \tag{A.6}$$

$$\Sigma_2 = \sum_{m=-\infty}^{\infty} \frac{(q+mS)H_1^{(2)}(\varpi\sqrt{(q+mS)^2+\varsigma^2})}{\beta_x\sqrt{(q+mS)^2+\varsigma^2}} e^{i(q+mS)\delta} \tag{A.7}$$

$$\Sigma_3 = \sum_{m=-\infty}^{\infty} H_0^{(2)}(\varpi\sqrt{(q+mS)^2+\varsigma^2}) e^{i\delta(q+mS)} \tag{A.8}$$

and

$$\delta = \frac{\sigma}{S} - \kappa M\sin\theta$$

$$\varpi = \kappa\beta_x$$

$$\beta_x^2 = 1 - M^2 \cos^2 \theta$$

The major advatage by introduction of the new variables q and ς is that the Poisson summation formula can be used. For a sum $\sum_m F(mS+q)$ this states

$$\sum_{m=-\infty}^{\infty} F(mS+q) = \sum_{n=-\infty}^{\infty} e^{i\frac{2\pi n}{S}q} \frac{1}{S} \int_{-\infty}^{\infty} F(t) e^{-i\frac{2\pi n}{S}t}\, dt$$

The summation formula in conjunction with the knowledge of the Fourier transforms of the Hankel functions make it possible to convert the sums in K_p and K_w into series of exponential functions. The Fourier transforms that are needed can be found from an integral formula of Bessel functions in Gradshteyn and Ryzhik (1965)

$$\int_0^{\infty} J_\nu(\tau z) K_\mu(b\sqrt{z^2-\varpi^2})(z^2-\varpi^2)^{-\frac{\mu}{2}} z^{\nu+1}\, dz = \frac{\pi}{2} e^{-i\pi(\mu-\nu-\frac{1}{2})} \frac{\tau^\nu}{b^\mu} \{\frac{\sqrt{\tau^2+b^2}}{\varpi}\}^{\mu-\nu-1} \times$$

$$\times H^{(2)}_{\mu-\nu-1}(\varpi\sqrt{\tau^2+b^2}) \tag{A.9}$$

where J_ν and K_μ are Bessel function and modified Bessel function respectively. By using ν and μ of $\pm\frac{1}{2}$ and the inverse of the Fourier transform the following relations may be obtained

$$\int_0^{\infty} \frac{H_1^{(2)}(\varpi\sqrt{\tau^2+b^2})}{\sqrt{\tau^2+b^2}} \cos(z\tau) d\tau = \frac{i e^{-b\sqrt{z^2-\varpi^2}}}{b\varpi} \tag{A.10}$$

$$\int_0^{\infty} \frac{\tau H_1^{(2)}(\varpi\sqrt{\tau^2+b^2})}{\sqrt{\tau^2+b^2}} \sin(z\tau) d\tau = \frac{i z e^{-b\sqrt{z^2-\varpi^2}}}{\varpi\sqrt{z^2-\varpi^2}} \tag{A.11}$$

$$\int_0^{\infty} H_0^{(2)}(\varpi\sqrt{\tau^2+b^2}) \cos(z\tau) d\tau = \frac{i e^{-b\sqrt{z^2-\varpi^2}}}{\sqrt{z^2-\varpi^2}} \tag{A.12}$$

Now the series in the kernel functions can be converted to

$$\Sigma_1 = \frac{2i}{S\varpi\varsigma} \sum_{n=-\infty}^{\infty} e^{i\frac{2\pi n}{S}q - \varsigma\sqrt{(\delta-\frac{2\pi n}{S})^2-\varpi^2}} \tag{A.13}$$

$$\Sigma_2 = \frac{2}{S\varpi} \sum_{n=-\infty}^{\infty} \frac{(\frac{2\pi n}{S}-\delta)}{\sqrt{(\delta-\frac{2\pi n}{S})^2-\varpi^2}} e^{i\frac{2\pi n}{S}q - \varsigma\sqrt{(\delta-\frac{2\pi n}{S})^2-\varpi^2}} \tag{A.14}$$

$$\Sigma_3 = \frac{2i}{S} \sum_{n=-\infty}^{\infty} \frac{e^{i\frac{2\pi n}{S}q - \zeta\sqrt{(\delta - \frac{2\pi n}{S})^2 - \varpi^2}}}{\sqrt{(\delta - \frac{2\pi n}{S})^2 - \varpi^2}} \tag{A.15}$$

Substituting Σ_3 in the integral in the equation for K_w and the integration carrying out we find the following result for a field point lying upstream of the doublets:

$$\Sigma_4 = \frac{2i}{S} \sum_{n=-\infty}^{\infty} \int_{-\infty}^{\infty} e^{\frac{i\lambda}{\beta^2}(x_1' - \xi)} \frac{e^{i\frac{2\pi n}{S}q - \zeta\sqrt{(\delta - \frac{2\pi n}{S})^2 - \varpi^2}}}{\sqrt{(\delta - \frac{2\pi n}{S})^2 - \varpi^2}} dx_1' =$$

$$= \frac{2i}{S} \sum_{n=-\infty}^{\infty} e^{i\frac{\lambda}{\beta^2}(x_1 - \xi)} \frac{e^{i\frac{2\pi n}{S}q - \zeta\sqrt{(\delta - \frac{2\pi n}{S})^2 - \varpi^2}}}{\sqrt{(\delta - \frac{2\pi n}{S})^2 - \varpi^2}\,\{i(\frac{2\pi n}{S} - \delta)q_x + i\frac{\lambda}{\beta^2} + \zeta_x\sqrt{(\delta - \frac{2\pi n}{S})^2 - \varpi^2}\}} \tag{A.16}$$

for $(x_1 - \xi)\cos\theta - y_1 \sin\theta < 0$.

For a field point downstream of the doublets we find:

$$\Sigma_4 = \frac{2i}{S} \sum_{n=-\infty}^{\infty} \int_{-\infty}^{\infty} e^{\frac{i\lambda}{\beta^2}(x_1' - \xi)} \frac{e^{i\frac{2\pi n}{S}q - \zeta\sqrt{(\delta - \frac{2\pi n}{S})^2 - \varpi^2}}}{\sqrt{(\delta - \frac{2\pi n}{S})^2 - \varpi^2}} dx_1' =$$

$$= \frac{2i}{S} \sum_{n=-\infty}^{\infty} e^{i\frac{\lambda}{\beta^2}(x_1 - \xi)} \frac{e^{i\frac{2\pi n}{S}q - \zeta\sqrt{(\delta - \frac{2\pi n}{S})^2 - \varpi^2}}}{\sqrt{(\delta - \frac{2\pi n}{S})^2 - \varpi^2}\,\{i(\frac{2\pi n}{S} - \delta)q_x + i\frac{\lambda}{\beta^2} - \zeta_x\sqrt{(\delta - \frac{2\pi n}{S})^2 - \varpi^2}\}} +$$

$$+ \frac{i4\zeta_x}{S} e^{i\frac{\lambda y_1 \tan\theta}{\beta^2}} \sum_{n=-\infty}^{\infty} \frac{e^{-i\frac{(2\pi n - S\delta)y_1}{S\cos\theta}}}{\{(\frac{2\pi n}{S} - \delta)q_x + \frac{\lambda}{\beta^2}\}^2 + \zeta_x^2\{(\delta - \frac{2\pi n}{S})^2 - \varpi^2\}} \tag{A.17}$$

where q_x and ζ_x are

$$q_x = -\frac{\sin\theta}{\beta_x^2}$$

$$\zeta_x = \frac{\beta\cos\theta}{\beta_x^2}$$

The second term in this equation is the vortical velocity component normal to the blade surface, so it represents the vorticity wave shed by the blade.

By introducing

$$\mu_n = \frac{2\pi n + \sigma}{S}$$

$$\alpha_{1,2} = \frac{1}{\beta_x^2}\{M_x(M_y\mu_n + \lambda M) \pm \sqrt{(M_y\mu_n + \lambda M)^2 - \beta_x^2\mu_n^2}\}$$

where

$$M_x = M\cos\theta \quad \text{and} \quad M_y = M\sin\theta$$

one can write the kernel functions in the following forms, which are the same expressions as Smith (1971) and Ni (1979) derived by using a different approach.

$$K_p = -\sum_{n=-\infty}^{\infty} \frac{\mu_n\cos\theta - \alpha_{1n}\sin\theta}{S\beta_x^2(\alpha_{2n} - \alpha_{1n})} e^{i(\alpha_{1n}\cos\theta + \mu_n\sin\theta)(x_1-\xi) - i(\alpha_{1n}\sin\theta - \mu_n\cos\theta)y_1} \tag{A.18}$$

$$K_w = \sum_{n=-\infty}^{\infty} \frac{(\mu_n\cos\theta - \alpha_{1n}\sin\theta)^2}{S\beta_x^2(\alpha_{2n} - \alpha_{1n})(\lambda + \alpha_{1n}\cos\theta + \mu_n\sin\theta)} \times$$

$$\times\, e^{i(\alpha_{1n}\cos\theta + \mu_n\sin\theta)(x_1-\xi) - i(\alpha_{1n}\sin\theta - \mu_n\cos\theta)y_1} \tag{A.19}$$

For $(x_1 - \xi)\cos\theta - y_1\sin\theta < 0$, and

$$K_p = -\sum_{n=-\infty}^{\infty} \frac{\mu_n\cos\theta - \alpha_{2n}\sin\theta}{S\beta_x^2(\alpha_{2n} - \alpha_{1n})} e^{i(\alpha_{2n}\cos\theta + \mu_n\sin\theta)(x_1-\xi) - i(\alpha_{2n}\sin\theta - \mu_n\cos\theta)y_1} \tag{A.20}$$

$$K_w = \sum_{n=-\infty}^{\infty} \frac{(\mu_n\cos\theta - \alpha_{2n}\sin\theta)^2}{S\beta_x^2(\alpha_{2n} - \alpha_{1n})(\lambda + \alpha_{2n}\cos\theta + \mu_n\sin\theta)} e^{i(\alpha_{2n}\cos\theta + \mu_n\sin\theta)(x_1-\xi)} \times$$

$$\times\, e^{-i(\alpha_{2n}\sin\theta - \mu_n\cos\theta)y_1} - \sum_{n=-\infty}^{\infty} \frac{\lambda^2\cos\theta}{S(\lambda^2 + \mu^2 + 2\lambda\mu\sin\theta)} e^{-i\lambda(x_1-\xi) + i\frac{\lambda\sin\theta + \mu_n}{\cos\theta}y_1} \tag{A.21}$$

for $(x_1 - \xi)\cos\theta - y_1\sin\theta > 0$.